

LNF - 64/6
16.3.1964.

C. Bacci, C. Mencuccini, G. Penso, R. Querzoli, G. Salvini,
V. Silvestrini and A. Wattenberg: PHOTOPRODUCTION AND
NEUTRAL DECAY MODES OF THE η -PARTICLE. -

(Nota interna : n. 234)

Nota interna: n. 234

16 Marzo 1964.

C. Bacci^(x), C. Mencuccini, G. Penso^(x), R. Querzoli, G. Salvini^(x),
V. Silvestrini and A. Wattenberg^(o): PHOTOPRODUCTION AND
NEUTRAL DECAY MODES OF THE η -PARTICLE.

INTRODUCTION. -

The η -particle⁽¹⁻⁸⁾ is one of the most complicated and under many respects interesting objects among the pion resonances discovered in the last few years. The modes of decay of this particle, as well as the behaviour of the production cross section are encouraging subjects for further study, both experimental and theoretical.

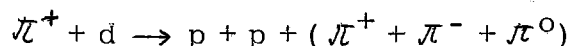
The present paper deals with the neutral decay modes of the η , and in particular with the results of an experiment that we have carried out by studying the photoproduction reaction



at the Frascati 1.1 GeV electron-synchrotron.

We give in this section a short historical introduction and a synthesis of our present results.

a) The η was discovered by Pevsner and coworkers⁽¹⁾. The authors observed a 546 MeV mass (with a width ≤ 25 MeV) decaying into 3 π 's, while studying the reaction



Confirmation came rather soon from the analysis of the reactions $K^- + p \rightarrow \Lambda^0 + (\pi^+ + \pi^- + \pi^0)$; $K^- + p \rightarrow \Lambda^0 + \text{neutrals}$ ⁽²⁾; and from other reactions⁽³⁻⁸⁾. It was soon clear that the η prefers to decay into neutral modes (π^0 's and γ 's) rather than into the charged $\pi^+ \pi^- \pi^0$ mode, and the value of the branching ratio A ^(1, 2, 8, 9) has been measured to be, with some difference among different groups

(x) - Istituto di Fisica dell'Università di Roma, and Istituto Nazionale di Fisica Nucleare, Sezione di Roma, Roma, Italy

(o) - National Science Foundation Fellow, on leave from the University of Illinois, Urbana, Illinois, USA.

$$A = \frac{\Gamma(\text{all neutral modes})}{\Gamma(\pi^+ + \pi^- + \pi^0)} = 2.5 \pm .4$$

The search for a charged η , for instance with a decay $\pi^\pm + \pi^\pm + \pi^\mp$, has been unsuccessful⁽¹⁰⁾, so that an isospin value $T=0$ has been generally accepted.

The abundance of the neutral decays, as well as the fact that the decay $\rho \rightarrow \eta + \pi$ is not observed⁽¹¹⁾, soon gave rise to the hypothesis, now rather well confirmed by other experiments and by the present research, that the decay $\pi^+ + \pi^- + \pi^0$ occurs with a violation of G-parity.

The presence of a radiative decay mode was thus strongly suggested, as well as the assumption that the decays into 3 pions proceed via an electromagnetic process of order α^2 .

The first evidence of a non pionic neutral decay of the η came from a measurement with the Frascati synchrotron, which was reported by us at the Geneva Conference 1962⁽¹²⁾. We observed a radiative decay mode of the η which we interpreted either as a $\pi^0 + \gamma$ or a $\gamma + \gamma$ mode, and which now, from other direct and indirect evidence, appears clearly to be a $\gamma + \gamma$ mode⁽¹³⁾.

The proceedings of the Geneva Conference 1962 provide information on the experimental situation on the η , as of June 1962. At that time, mostly on the basis of the Dalitz plot, the η was already clothed in its quantum numbers, which are now rather definitely confirmed: $J=0, I=0; P=-1; G=+1$, that is $J^{P,G} = 0^{-+}$.

These are the quantum numbers at production, while the η decays either through G parity violation into the final state 0^{--} , or in a radiative mode.

Between the 1962 Geneva meeting and the present time, the following experimental informations have become available:

- The non pionic decay mode observed in photoproduction⁽¹²⁾ has been identified, as we said, as a $\gamma + \gamma$ mode⁽¹³⁾ (in agreement with $J=0$).
- The mass has been well localized as $m_\eta = 548 \pm 1$ MeV⁽⁸⁾; this is the mean value, the full width Δm still being in the experimental limit $\Delta m \leq 10$ MeV⁽⁸⁾.
- The mode $\pi^+ + \pi^- + \gamma$, which had not been observed before, is observed by Fowler and cow. with a branching ratio

$$\frac{\Gamma(\pi^+ + \pi^- + \gamma)}{\Gamma(\pi^+ + \pi^- + \pi^0)} \approx 0.26 \pm 0.08^{(9)}$$

- A second neutral decay mode, that is the $\eta \rightarrow \pi^0 + \pi^0 + \pi^0$, has been observed; this was reported by our group at the Cambridge Conference on Photon Interactions in the BeV-energy Range⁽¹⁴⁾, and was found by Crawford and cow.⁽¹⁵⁾ by direct inspection of the electron pairs in the Berkeley H₂ Bubble Chamber. There is now rather general agreement that the most important decays of the η should be the ones we mentioned:

$$\pi^+ + \pi^- + \pi^0; \quad \gamma + \gamma; \quad \pi^0 + \pi^0 + \pi^0; \quad \pi^+ + \pi^- + \gamma.$$

The mode $\pi^0 + \gamma + \gamma$ is not forbidden, and its existence is not excluded by experiments until now.

b) Since its discovery a quite large theoretical literature flourished around the η . One of the interesting properties of this particle is the possibility it has to decay with comparable frequencies in pionic as well as in radiative ways. The theoretical connection between the various decay modes of the η is still an open problem. Several different theoretical models have been proposed, and shall be examined and quoted by us in section 7. The aim of the models is mainly speculation on the following points:

I - The relevant abundance of the three pion decay mode relative to $\eta \rightarrow 2\gamma$ and also to $\eta \rightarrow \pi^+ + \pi^- + \gamma$; in fact the decay of η into 3π , which violates the G-parity conservation law, can proceed only via two virtual electromagnetic interactions; as a consequence, the $\eta \rightarrow 3\pi$ and the $\eta \rightarrow 2\gamma$ modes occur in the same electromagnetic order α^2 . In this scheme the 2γ mode would be enhanced with respect to the 3π one by a phase space factor of the order of 10^2 . The experiments indicate on the contrary $\Gamma(2\gamma) \approx \Gamma(3\pi)$.

II - The Dalitz plot density for the $\eta \rightarrow \pi^+ + \pi^- + \pi^0$ decay; in fact the simplest matrix element for the case of a three pion decay of a 0^{-+} particle, is a constant. The experimental information till now available shows quite clearly that the Dalitz plot for $\eta \rightarrow \pi^+ + \pi^- + \pi^0$ is not uniform, but rather favors the neutral pions of lower energy.

III - The value of the ratio $\Gamma(3\pi^0) / \Gamma(\pi^+ \pi^- \pi^0)$; this ratio depends on the final state interactions of the pions (See § 7).

IV - The value of the ratio $\Gamma(\pi^+ \pi^- \gamma) / \Gamma(\gamma \gamma)$; in fact, on the basis only of α power dependence arguments one would expect a factor of the order of α between the $\pi^+ + \pi^- + \gamma$ mode (occurring in electromagnetic order α) and the $\gamma + \gamma$ mode (of order α^2). The experimental value is

$$\Gamma(\pi^+ + \pi^- + \gamma) / \Gamma(\gamma + \gamma) \simeq 6/31 \simeq 1/5.$$

V - The value of the partial rate of the $\eta \rightarrow \pi^0 + \gamma + \gamma$ mode with respect to the other decay modes (See § 4 and § 7).

VI - The absolute width of the η . The experimental width Δm is of the order of 8 MeV, due to the instrumental resolution, while theory indicates that the width should not exceed one keV (See § 7).

It is worth noticing that the possible leptonic decay modes of the η (of the type $\pi^0 + e^+ + e^-$; $\pi^0 + \mu^+ + \mu^-$) are of order α^4 and can be considered negligible in the present experimental situation.

c) We have observed the process (1) of photoproduction of the η particle at 978 and 939 MeV, using the 1100 MeV Frascati electron synchrotron, and a technique of spark chamber, scintillation and Cerenkov counters. The experimental method (we have really employed two rather independent methods) and the procedure we used to separate the multipion background from the η are described in Sections 2 and 3.

The experimental results, that is the counting rates and energy spectra obtained with our apparatus, are reported in Section 3, and in figs. 6 to 11.

The branching ratio of the $\gamma + \gamma$ decay mode relative to other neutral modes has been evaluated in the two ways reported in Section 4, and

4.

Table I. If we assume from the theory that the $\pi^0 + \gamma + \gamma$ mode is negligible, the other neutral mode beyond $\gamma + \gamma$ is the $3\pi^0$ decay, and we find from our measurements the branching ratio:

$$R = \frac{\Gamma(\gamma + \gamma)}{\Gamma(3\pi^0)} = .8 \pm .25 .$$

Through a comparison with other authors, we can list, although with large errors, the percentages for the various decay modes of the η (See Table II and Section 5).

In Section 7 the values of the branching ratios are compared with some of the current decay models. The situation will be summarized in Table IV.

The differential production cross section for process (1) is estimated in Section 6.

We considered convenient to add an Appendix 1 where the possible sources of errors and some of our difficulties are discussed and an Appendix 2 giving details on the calibration of the lead glass Cerenkov counter.

Our results have been already briefly reported in a preliminary note⁽¹⁶⁾.

Section 1 - EXPERIMENTAL METHOD. -

The experimental arrangement is shown in fig. 1.

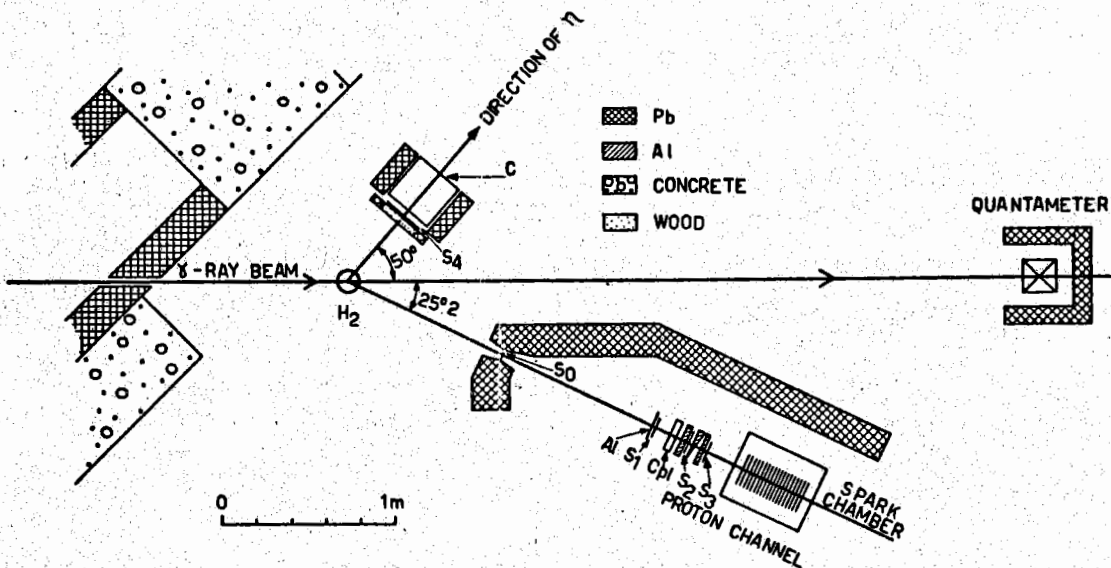


FIG. 1 - Experimental arrangement. C, lead glass Cerenkov counter to detect γ -rays. S, scintillation counters. The absorbers in the proton channel are Al.

The γ ray beam from the electron synchrotron hits the liquid hydrogen target, H_2 . This target is a vertical cylinder with a diameter of 7 cm. The beam intensity was monitored by a Wilson Quantameter⁽¹⁷⁾.

The proton channel P detects the recoil protons from reaction (1) at an angle $25.2^\circ \pm 1.3^\circ$ in the laboratory (the angular position of each

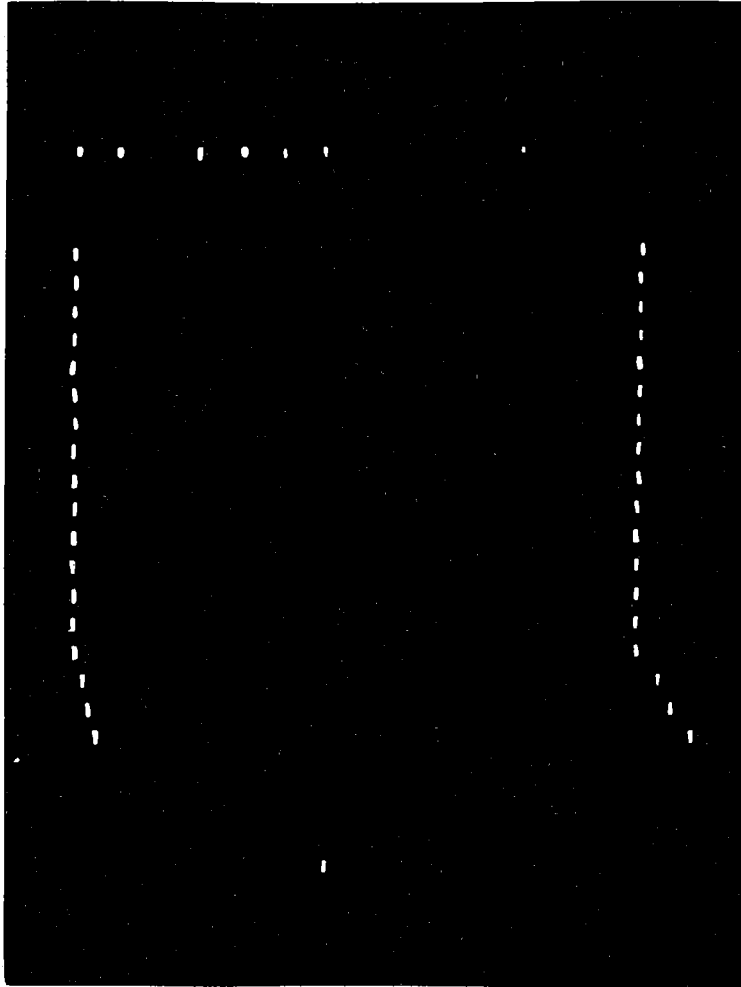


FIG. 2

A TYPICAL PHOTO OF THE SPARK CHAMBER. THE ROW OF SPOTS IN THE UPPER PART (LEFT) GIVES THE PULSE HEIGHT IN C. (64 CHANNELS IN BINARY FORM).

proton could be identified with an uncertainty of $\pm 3^\circ$). The energy of the protons is measured by their range in the spark chamber (S. C.).

The S. C. has useful volume $16 \times 16 \times 20 \text{ cm}^3$; it is formed by 19 aluminum plates 6 mm thick; the width of the gap between the plates is 6 mm. The chamber is filled with neon at 0.8 atm; the neon is kept pure by continuously circulating it through hot calcium by means of a thermosyphon system.

A mirror optical system allows two 90° views of the spark chamber and consequently the spacial reconstruction of the events; the high voltage pulse to the spark chamber is supplied through a spark gap in air.

The proton telescope system contains a plexiglass Cerenkov counter in anticoincidence (labelled Cpl), in order to eliminate most of the pions. To be sure that after this there is no important pion contamination, a pulse height analysis was made in two of the scintillation counters of the telescope, taking into account that, for a given range, protons have a specific ionization which is about twice as large as the specific ionization of the pions. This test made us confident that there is practically no pion contamination in our measurements.

On the line of flight of the η , there is a total absorption lead glass Cerenkov counter, C, to detect γ -rays in coincidence with the recoil protons; an anticoincidence counter, S_4 , shielded by 6.5 g/cm^2 wood is in front of C. The energy of the γ rays detected by C is measured by a pulse height analyzer and recorded on the photograph of the spark chamber by means of neon lamps. γ -rays with energy $< 200 \text{ MeV}$ do not trigger the spark chamber. An example of the photographs is given in fig. 2. The pulse height versus energy calibration of C was made with a monochromatic electron beam, selected by the Frascati pair spectrometer⁽¹⁸⁾. Some detail on this point is given in Appendix 2.

Specifically, in order to get the events of a proton plus a γ in the Cerenkov C, we detected and analyzed in C and in the spark chamber all the events:

$$(2) \quad S_0 + S_1 + S_2 + S_3 - C_{pl} - S_4 + C$$

We shall indicate briefly all these coincidences in the following as P+C.

A block diagram of the electronics is reported in fig. 3

The absorbers in the proton telescope are Aluminum. The wedge shaped shim between S_2 and S_3 corrects for the angular dependence of the proton energy.

The range energy relations for the protons are taken from the Berkeley Tables (U. C. R. L. 2301).

With the geometrical arrangement and the absorbers chosen, we can detect the events due to the reaction (1). This can be done essentially by two different methods, which are briefly described:

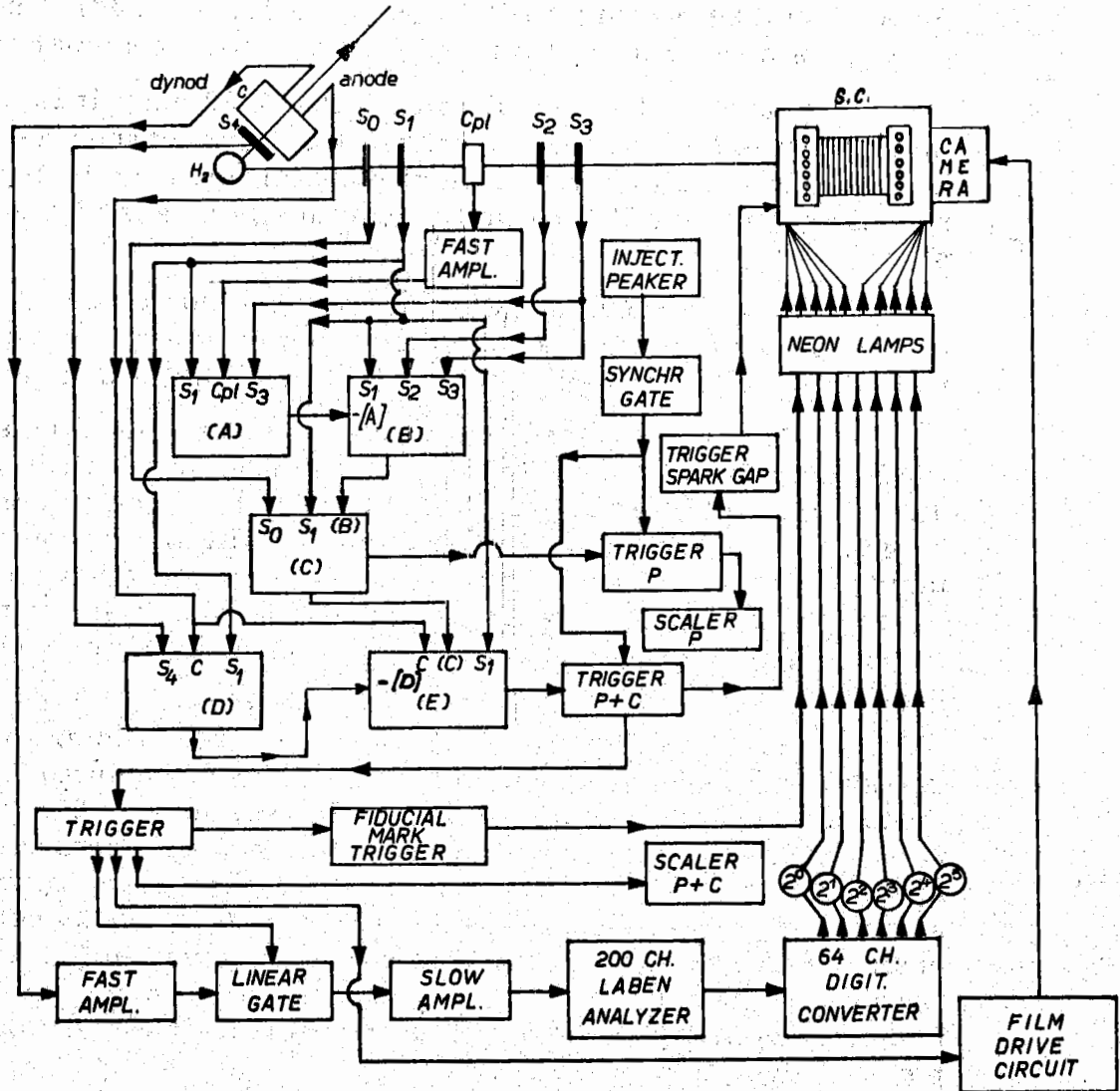


FIG. 3 - Block diagram of the electronics of the experiment.

a) The step method.

From a two body process like (1), the energy of the recoil proton, at a given angle, is function only of the energy of the primary photon. Therefore, the energy spectrum of the protons from reaction (1) is in a given direction an "image" of the bremsstrahlung spectrum (weighted with the cross section for process (1)).

The energy E_0 of the synchrotron and the absorbers in the proton telescope are chosen in the step method in such a way that the image of the end of the bremsstrahlung spectrum falls in the center of the spark chamber. When one plots the number of protons as a function of their energy, a step should appear in the center of the chamber due to reaction (1). The step should be as steep as allowed by the shape of the bremsstrahlung spectrum near its maximum energy. The step will be more evident if the differential cross section $d\sigma/d\Omega$ remains rather constant versus the energy of

the primary γ -ray over an interval of 20-30 MeV; this assumption has not been contradicted by the experiment.

In fig. 4, in order to make this point more clear, we have reported the step due to the reaction $\gamma + p \rightarrow \pi^0 + p$. This was obtained without changing the absorbers in the proton telescope with respect to the η -measurements: the energy of the synchrotron was lowered to 660 MeV, and the Cerenkov C was placed at the proper angle (100°).

In this case the kinematics is such that the position of the step is rather insensitive on the mass of the π^0 and sharply dependent on the energy E_0 of the synchrotron. We obtain in this way a check of the calibration of the nominal energy of the synchrotron, and detailed informations on the shape of the end of the bremsstrahlung spectrum (we know that the single π^0 production cross section is rather constant around 660 MeV).

In figs. 6a and 6b, a typical η -step is shown (See Section 3). In this case the step appears on a background due to multipion production. The position of the step is for the η rather sensitive to its mass. The step of fig. 6b corresponds to a mass of the η of 550 ± 10 MeV. From this height of the step the differential cross section for process (1) can be deduced.

The details of this figure and the results obtained with the step method are discussed later.

b) The γ -method.

This method has been already used by us in a previous experiment⁽¹²⁾: we fix a relatively small energy band of the protons and look at the spectrum of the γ -rays detected in the Cerenkov C when there is a coincidence (2). The energy bands of the protons are selected by the S. C.

Of course, other processes than $\gamma + p \rightarrow \eta + p$ can give coincidences of the proton channel with a γ -ray (coincidence (2)) and in particular the processes

$$(3a) \quad \gamma + p \rightarrow 2\pi^0 + p$$

$$(3b) \quad \gamma + p \rightarrow \pi^0 + p + \text{many pions} .$$

None of these processes give rise to mass steps in the proton spectra, and they must exhibit a smooth γ ray spectrum, due to the origin of these γ 's from π^0 's originated in multipion processes.

In fig. 5 we report the shape of the γ -ray spectra as expected on the Cerenkov C (See fig. 1) in different cases, under the following hypothesis: the recoil proton is emitted at a laboratory angle $\theta_p = 25.2^\circ$ with a kinetic energy $T_p = 278$ MeV; the bremsstrahlung spectrum has a maximum energy of 1000 MeV.

Specifically, curves $\phi_1, \phi_2, \phi_3, \phi_4$ have the following meaning: ϕ_1, γ spectrum on C from the reaction (1), when $\eta \rightarrow \gamma + \gamma$. Of these two γ -rays, only one can enter the Cerenkov due to the kinematical conditions.

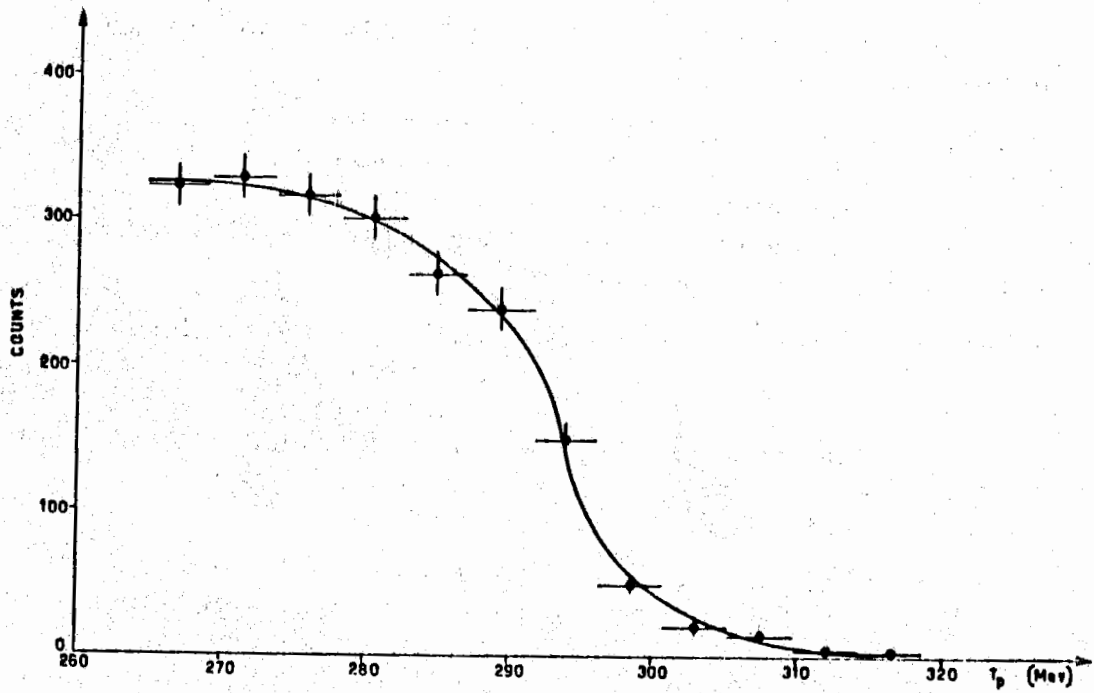


FIG. 4 - The step in the S. C. in the reaction $\gamma + p \rightarrow \pi^0 + p$. Ordinates: number of protons observed. Abscissae: kinetic energy of the protons. Nominal energy of the electronsynchrotron, 660 MeV. The results are corrected for nuclear interactions.

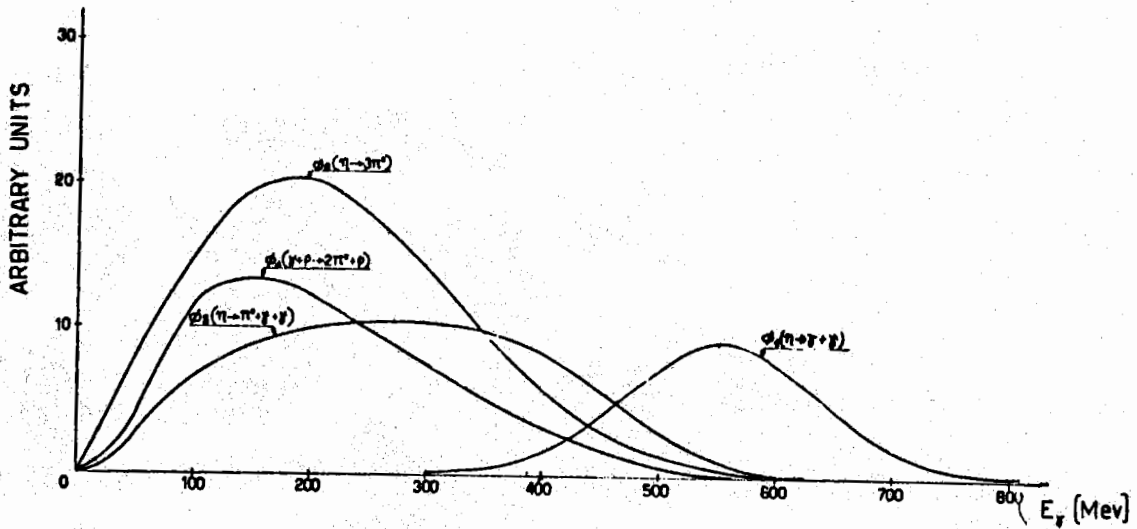


FIG. 5 - Shape of the γ -ray spectra as expected on the Cerenkov C in different cases: ϕ_1 : $\gamma + p \rightarrow \pi + p$, $\gamma \rightarrow \gamma + \gamma$; ϕ_2 : $\gamma + p \rightarrow \pi + p$, $\gamma \rightarrow \pi^0 + \pi^0 + \pi^0$; ϕ_3 : $\gamma + p \rightarrow \pi + p$, $\gamma \rightarrow \pi^0 + \gamma + \gamma$; ϕ_4 : $\gamma + p \rightarrow \pi^0 + \pi^0 + p$. In all cases $\theta_p = 25.2^\circ$; $T_p = 280$ MeV; maximum energy of the incident bremsstrahlung spectrum 1000 MeV. Curves ϕ_1 , ϕ_2 , ϕ_3 may be compared: they refer to the same number of π 's under the hypothesis that the branching ratios among the three decay modes are 1 : 1 : 1.

- ϕ_2 , same, in the case $\eta \rightarrow 3\pi^0$. In computing ϕ_2 as well as ϕ_3 , ϕ_4 , we have included the contribution due to more than one γ -ray entering C.
- ϕ_3 , same, in the case $\eta \rightarrow \pi^0 + \gamma + \gamma$.
- ϕ_4 , γ -ray spectrum from the reaction $\gamma + p \rightarrow \pi^0 + \pi^0 + p$ under the hypothesis of a cross section constant with the energy of the primary γ -rays.

The distributions ϕ_2 , ϕ_3 , ϕ_4 have been calculated on the basis of a non invariant statistical model(19).

This model is not as crude as one could think: in fact we have checked that the γ spectrum is widely insensitive to possible modifications of the π^0 spectrum, due for instance to final state interaction.

The curves ϕ_2 , ϕ_3 , ϕ_4 may be directly compared: they refer to the same number of η 's, under the hypothesis that the branching ratio among the three decay modes are 1:1:1. In spectra ϕ_1 , ϕ_2 , ϕ_3 , ϕ_4 the experimental resolution was folded-in.

It is clear from fig. 5 that the η decay into $\gamma + \gamma$ is rather clearly distinguishable from the other processes. We shall see however that by using both methods (a) and (b), we can get informations also on the other neutral decay modes of the η .

The evaluation of the contribution of processes (3), the background events, is the main problem to be solved before we can obtain quantitative informations on the η -photoproduction.

Before going into the details of the two methods outlined, the evaluation of the multipion background is discussed in the following section.

Section 2 - EVALUATION OF THE MULTIPION BACKGROUND. -

The π^0 's from single photoproduction are excluded by our geometry and energy requirements. In fact the γ 's from single π^0 's, at the angle of our Cerenkov would have an energy ≤ 100 MeV.

To evaluate the contribution of processes (3), we have systematically collected experimental data in kinematical conditions in which the η could not be produced, but as close as possible to our η threshold. The many measurements we did below the η -threshold allow us to construct on an experimental basis the piece of the phase space function (weighted by the experimental efficiency) for the processes (3) in the kinematical region where the η is excluded. This function has been extrapolated to the η region: the contamination of processes (3) to the η measurements was evaluated in this way.

Specifically the following was done: let us indicate by $N = N(E_0, T_p, E_\gamma)$ the number of P+C (coincidence (2)), due to processes (3) (multipion production), in which a proton of energy T_p is emitted at 25.2° as in our case, and a photon of energy E_γ enters the Cerenkov C. E_0 is the maximum energy of the bremsstrahlung spectrum producing the reaction (3). N is the number of coincidences P+C for given intervals ΔT_p and ΔE_γ . On the basis of our phase space calculations (those we used to draw fig. 5), the func-

tion N will have the following characteristics: (as long as the cross section for processes (3) does not change very drastically, as a function of the primary γ -ray energy):

a) The variable E_γ may be in good approximation considered separated by the other variables:

$$(4) \quad N = N(E_0, T_p) g(E_\gamma);$$

b) A moderate ($\approx 10\%$) increment of E_0 to $E_0 + \Delta E_0$ contributes to N a number of protons which is practically flat as a function of T_p . The function N (in the range of variation of the variables considered by us) must therefore have the form:

$$(5) \quad N = \left[F(T_p) + c \Delta E_0 \right] g(E_\gamma).$$

At this point we can determine $F(T_p)$, c , and $g(E_\gamma)$ by using our experimental results, and, what is more important, we can verify that the hypothesis we did are consistent with the experimental data.

$F(T_p)$ has been determined by the best fit (a function of the type $a + (b/T)^2$ was adequate) on the experimental results for $E_0 = 950$ MeV. The constant c comes from the comparison of the results for $E_0 = 900, 950, 1000$ MeV, through all the domain of T_p measured by us below the η threshold; $g(E_\gamma)$ was the best fit over one ($E_0 = 950$ MeV; $T_p = 278 \pm 17.5$ MeV) of the many distribution of E_γ we have at disposal in three independent series of measurements. We could verify that the other two distributions agree with the above hypothesis. At the end we obtained the function:

$$(6) \quad N = \left[-13.1 + 1.74 \times 10^6 / T_p^2 + 9.2 \times 10^{-2} (E_0 - 950) \right] g(E_\gamma)$$

where T_p and E_0 are expressed in MeV.

This rate (6) is referred to

$$\Delta T_p = 4.5 \text{ MeV} \quad \text{and a dosis of } 4.82 \times 10^{13} \text{ eq.}$$

As expected, the general agreement of (6) with all our experimental results is fairly good, making us confident a posteriori that the behaviour of the differential cross section for processes (3) is reasonably well behaved between 950 and 1000 MeV.

We can compare the results of this method with the usual procedure of calculating the multiplication background: specifically, with the aid of a 1620 IBM computer, we calculated the phase space distribution for the case of double production of π^0 's (reaction 3a)⁽²⁰⁾ on the hypothesis of the cross section being constant as a function of the energy of the primary γ . The general behaviour of N calculated in this way is very close to (5), (6), with the difference that with this model the increase of N with E_0 would be underestimated.

The function (6) gives us all the information we need about the multiplication background. Throughout the remainder of this paper, we shall suppose

that the behaviour of the background is correctly given by (6) including the region where the η is present.

It should be noted that the determination of the rate of the process



is rather insensitive to the behaviour of the background, which gives only a small contribution in the $\gamma + \gamma$ region.

Section 3 - EXPERIMENTAL RESULTS. -

a) Results with the step method. -

The experimental results with the step method are given in fig. 6 and fig. 7. Fig. 6a) gives the proton energy distribution (corrected for nuclear interactions) where the γ -ray detected in coincidence by C has an energy larger than 400 MeV. In this case all the η 's decaying in the $\gamma + \gamma$ mode with one of the two γ 's entering C are practically included (see the spectrum of these γ 's in fig. 5) and reactions (3) can give only a small contribution. In abscissae we report the kinetic energy of the protons stopping in the plates of our spark chamber (of a total of 18 gaps, we considered, to identify the proton and to determine its range, a total of 16 gaps, from the 2nd down to the 17th). In the ordinates the number of events per 4.82×10^{13} equivalent quanta is reported. Our results have been corrected for the nuclear interaction of the protons, in the absorbers and in the plates of the spark chamber, as usual in the range measurements of strongly interacting particles. The formula we used for such a correction is

$$N(R)_{\text{corr}} = \frac{N_{\text{meas}}(R) - N_{\text{meas}}(> R) \Delta R / \lambda}{e^{-R/\lambda}}$$

where:

- $N(R)$ is the number of protons having a range R ,
- $N(> R)$ is the number of protons with a range $> R$,
- ΔR is the thickness of a plate of the S. C.
- λ is the mean free path of the protons for nuclear interaction.

The value of λ used is

$$\lambda = 112 \text{ gr/cm}^2 \text{ Al}$$

as derived from the absorption total cross section measurements in Al done by G. P. Millburn et al. ⁽²¹⁾ with protons of energy 240 and 290 MeV (the absorption cross sections are quite independent on the energy in this energy region).

The solid lines in figg. 6a, 6c and 7a, 7c, are the contribution of reactions (3a), (3b), estimated by us using the method described in the previous section (the function (6) was integrated over $E_\gamma \geq 400$ MeV).

The difference between the experimental results and the solid line of fig. 6a gives in fig. 6b the step distribution of protons, as one expects from reaction (1) for $E_0 = 1000$ MeV. One sees that the mass of the η appears to be 550 ± 10 MeV in a good agreement with the known mass 548 ± 1

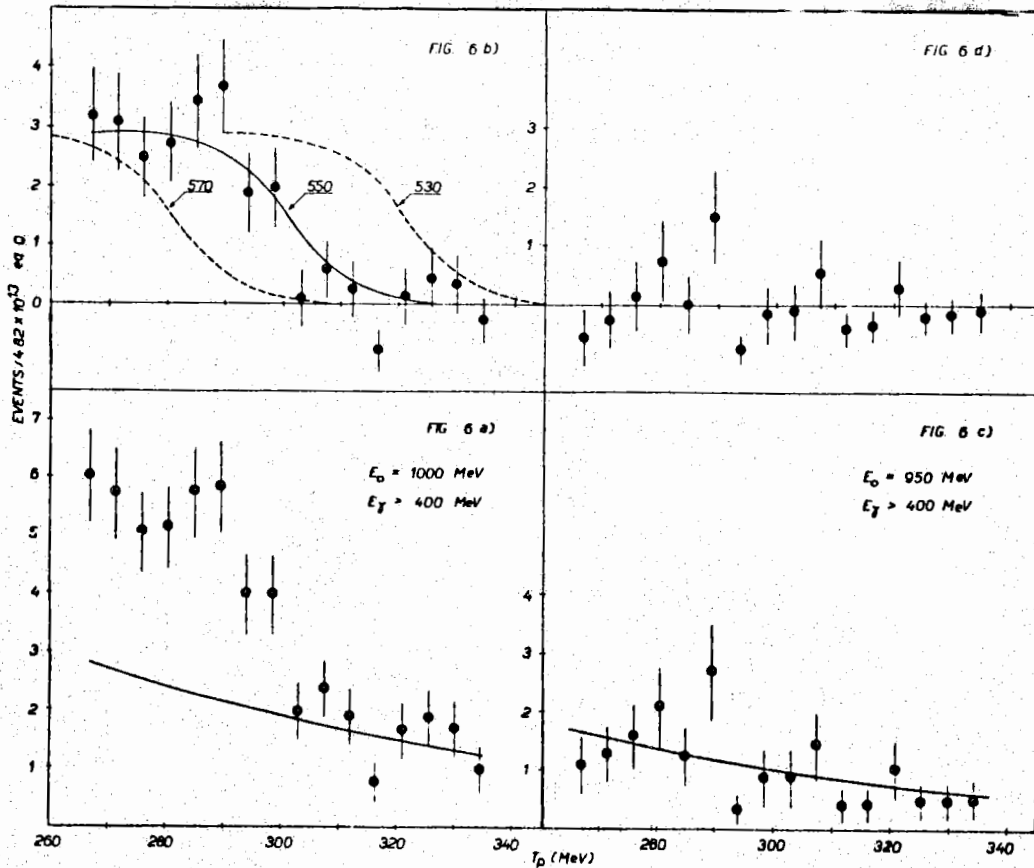


FIG. 6 - Energy spectra of protons in coincidence with η -rays of energy > 400 MeV. Abscissae: kinetic energy T_p (MeV) of the protons, as measured in the S. C.; ordinates: number of events in 4.82×10^{13} eq. Q. (a) The case when the process $\eta + p \rightarrow \eta + p$ is permitted kinematically; the solid line is the expected contribution from multi-pion processes. (b) The " η events", namely, the difference between the experimental points and the multi-pion background. The solid line is the expected shape of the proton spectrum from the process $\eta + p \rightarrow X^0 + p$ if X^0 has a mass of 550 MeV, that of the η . The dashed lines are for X^0 having a mass of 530 and 570 MeV. (c) and (d) Same as (a) and (b) except that the process $\eta + p \rightarrow \eta + p$ is forbidden kinematically. This is a null check.

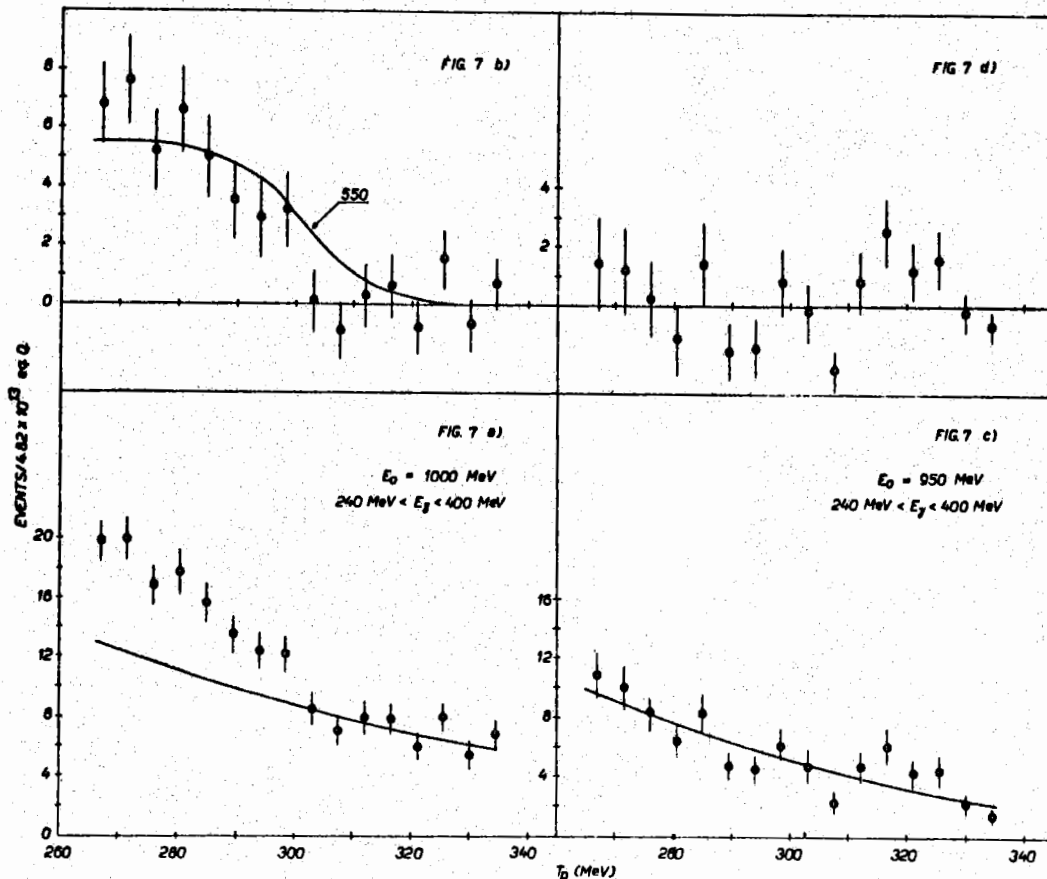


FIG. 7 - Energy spectra of protons in coincidence with η -rays of energy between 240 and 400 MeV. The step of (b) must be due to a three-body decay mode of the η (e. g. $\eta \rightarrow 3\pi^0$ and/or $\eta \rightarrow \pi^0 + \rho + \gamma$). (c) and (d) are again a null check.

MeV. The dotted lines refer to the masses 530, 570 MeV. This comparison makes us confident that we are really observing the η . The shape of the step (full line) in fig. 6b was evaluated experimentally, on the basis of the results already mentioned (photoproduction of π^0) and reported in fig. 4.

In figg. 6c, 6d, we applied the same procedure, but with the energy of the synchrotron lowered to 950 MeV, therefore with the step of the η removed out of the spark chamber. Figg. 6c and 6d do not exhibit any step; in fig. 6d the difference between the full line and the experimental points of fig. 6c are reported.

Figg. 7a, 7b, 7c and 7d have the same meaning as figg. 6a, 6b, 6c and 6d but now with the condition that $240 < E_\gamma < 400$ MeV, E_γ still being the energy of the photons detected by C. This measurements has been made in order to observe other neutral decay modes of the η , which exhibit rather different E_γ distribution, whose shapes are reported in fig. 5. The results are in this case more uncertain than before due to the increased contamination from reactions (3); so that the results of fig. 7 would not have constituted by themselves as convincing an evidence of the reaction (1) as they do when combined with the results of fig. 6.

The step of the η in the case of fig. 7b results from the η 's decaying in a different mode than in the $\gamma+\gamma$ mode, and as we shall see, our results agree with the hypothesis that this other mode is the decay of the η either in three π^0 's or in the mode $\eta \rightarrow \pi^0 + \gamma + \gamma$. The full lines are obtained also in this case by the function (6), integrated over E_γ from 240 MeV to 400 MeV.

Before calculating from the steps the neutral branching ratios of the η we present the results of the alternative way we used (the γ -method) to evidenciate the η photoproduction and to measure these same ratios.

b) Results with the γ -method. -

As we already mentioned in Section 1, this method consists in fixing a limited energy band of the protons, and looking at the γ -ray spectrum in the lead glass Cerenkov C (fig. 1). The results are given in figg. 8, 9, 10, 11. Fig. 8 refers to a distribution where the η 's are excluded by the kinematics: $E_0 = 950$ MeV, $T_p = 278 \pm 17.5$ MeV, $\theta_p = 25.2^\circ$. In this case, like in the other non η spectrum we have at our disposal, the distribution of the number of events versus E_γ is a smooth distribution.

The full line in fig. 8 is the best fit to the experimental points: in fact the function $g(E_\gamma)$ we put in (4), (5), (6) is just that of fig. 8.

The situation is different when the energy E_0 is increased, and the η is allowed by kinematics: the results for these cases are presented in figg. 9, 10, 11. We notice in these figures that it is impossible to fit the spectra with the simple distribution relative to the multipion processes (3), keeping also in mind that these distributions should come to an end around 600 MeV. Actually a good fit may be obtained only when a gaussian centered at 560 MeV is added to the monotonic distribution of the type shown in fig. 8.

We must note that in the case of fig. 11 the energy of the protons was 278 ± 17.5 MeV: the protons stopped in the spark chamber, and their

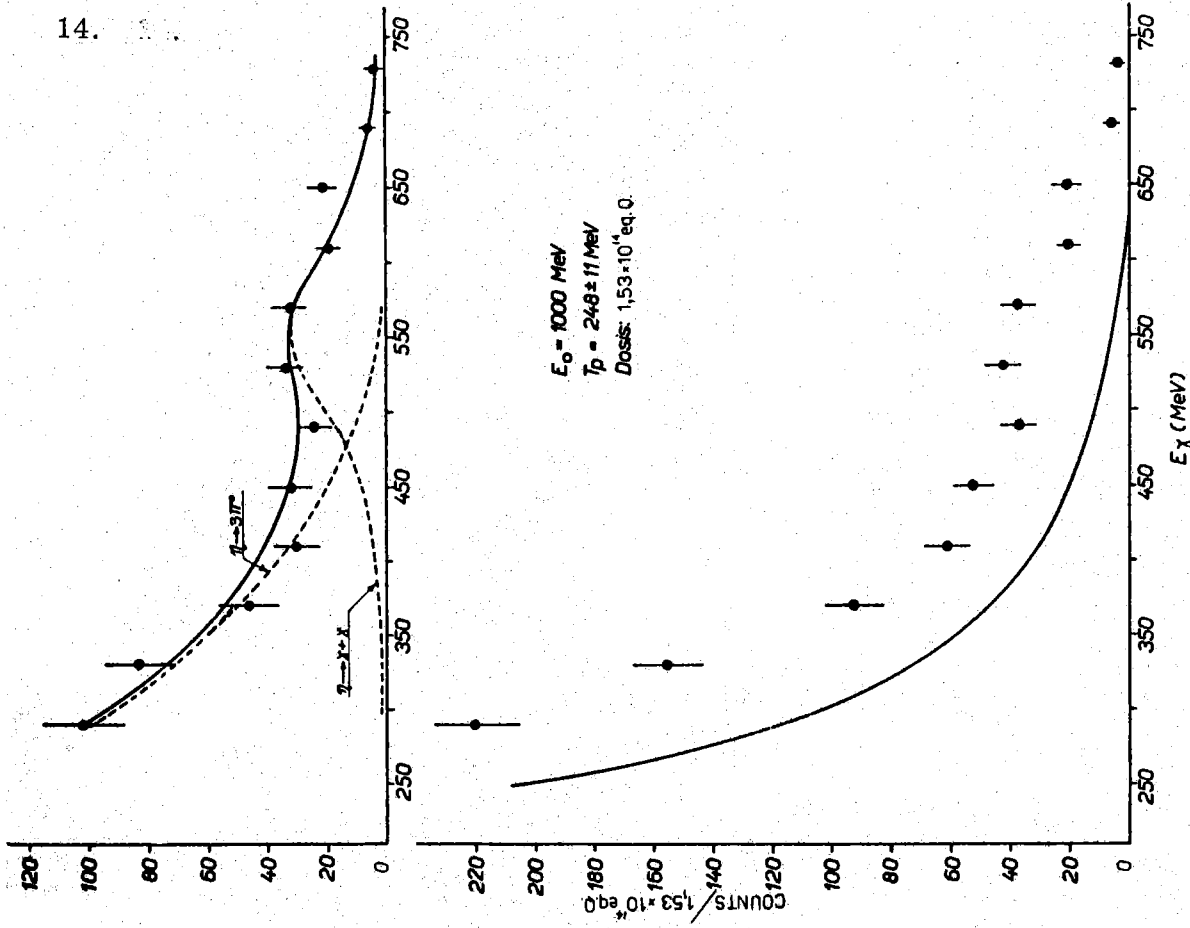


FIG. 9 - Spectrum obtained with the γ -ray method from the lead glass Ce-renkov detector. Abscissae: energy in MeV of the γ -ray detected in C. Ordinate: number of events in 1.53×10^{14} eq. Q. The solid line in the lower part of the figure is the expected contribution from multipion processes. The upper part shows the difference between the experimental points and the solid line. It is "best fitted" by a function of the form $a\beta_1 + b\beta_2$. See text.

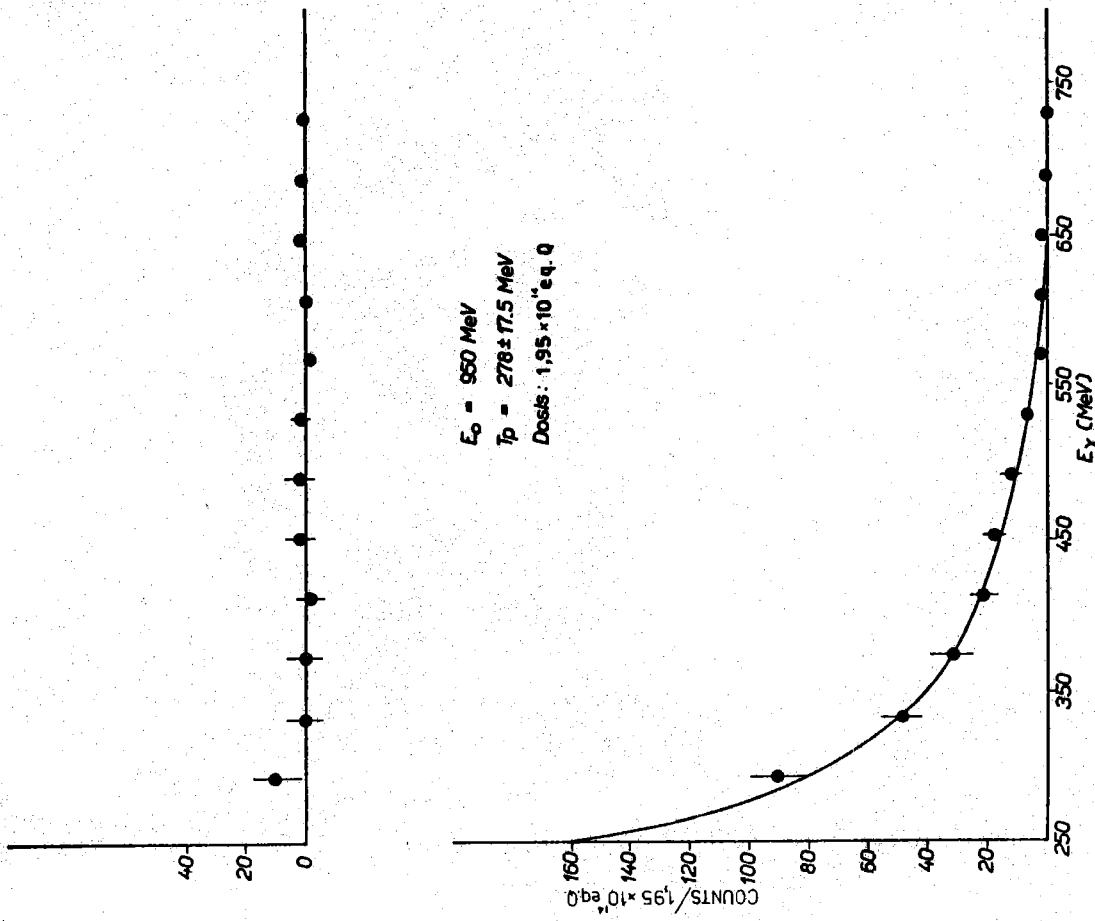


FIG. 8 - Spectrum obtained with the γ -ray method from the lead glass Ce-renkov detector. Abscissae: energy in MeV of the γ -ray detected in C. Ordinate: number of events in 1.95×10^{14} eq. Q. The solid line is the multipion contribution obtained by a best fit to the experimental points. The upper part of the figure shows the difference between the experimental points and the solid line. The figure shows a typical "non- γ spectrum".

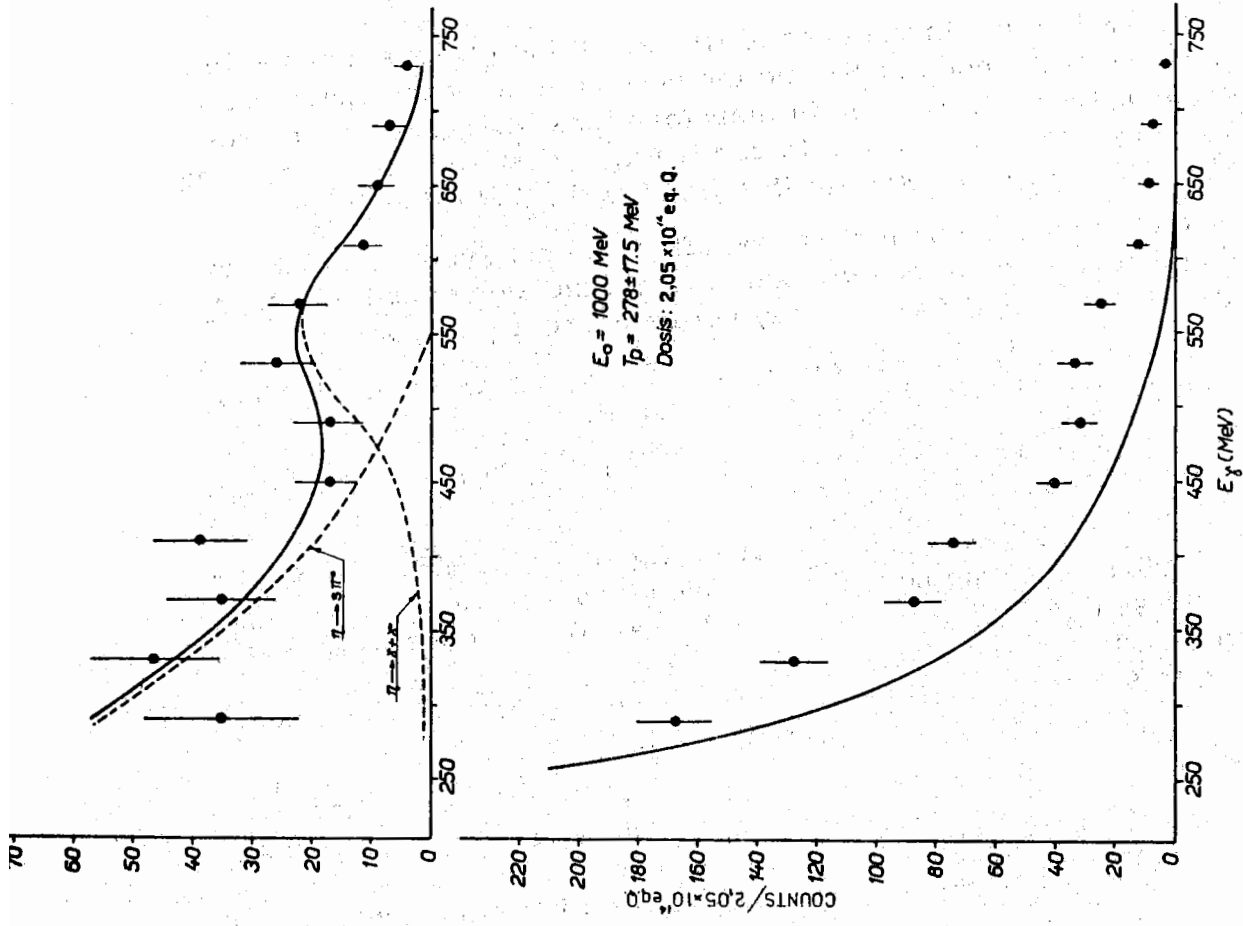


FIG. 11 - Spectrum obtained with the γ -ray method from the lead glass Ce-renkov detector. Abscissae: energy in MeV of the γ -ray detected in C. Ordinate: number of events in 2.05×10^{14} eq. Q. The solid line in the lower part of the figure and the points and lines of the upper part have the same meaning as in fig. 9.

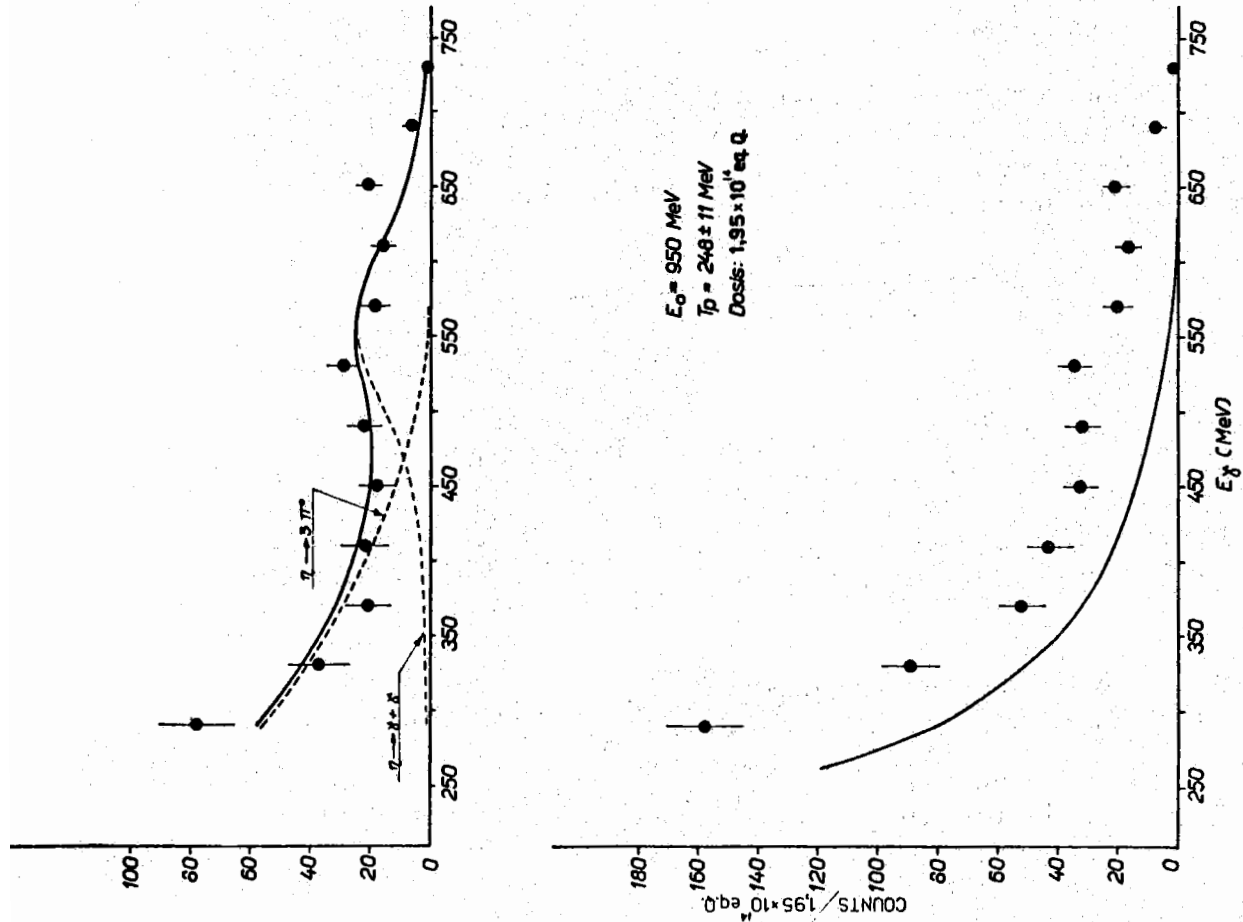


FIG. 10 - Spectrum obtained with the γ -ray method from the lead glass Ce-renkov detector. Abscissae: energy in MeV of the γ -ray detected in C. Ordinate: number of events in 1.95×10^{14} eq. Q. The solid line in the lower part of the figure and the points and lines of the upper part have the same meaning as in fig. 9.

tracks were clearly visible. In the case of fig: 9, 10 the protons stopped in the absorbers between the counter S_3 and the second plate of the spark chamber. The results of Fig. 9, 10 contain therefore less information, and some less control than those of fig. 11. In particular, the solid angle referring to those events is not very well known; this implies the following facts:

- a) the cross section for those points may be affected by a systematic error;
- b) the multipion contribution to be subtracted to get the events due to the process $\gamma + p \rightarrow \eta + p$ ($\eta \rightarrow 3\pi^0$) may not be correctly evaluated.

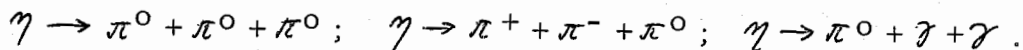
For this reasons, the values of R and of $d\sigma/d\Omega$ referring to those points have been put in parenthesis in Table I and III.

In order to obtain quantitative results on the η , from the curves 9, 10, 11, we have used the following procedure:

- using equation (6), with $g(E_\gamma)$ obtained from fig. 8 full line, we have calculated the contribution of the non- η processes (reaction (3)) to the E_γ distribution. These contributions are the full lines b), c), d) of fig. 9, 10, 11 in the lower part;
- by subtracting this multipion contribution from the experimental points, we have the three distributions 9, 10, 11 upper part.

These energy distributions are assigned by us to the photons coming from the decay of the η . These photons will have the energy distributions which we have already shown in fig. 5. The gaussian we just mentioned comes from the $\gamma + \gamma$ decay of the η , where the resolution in energy and angle of the Cerenkov C, and the energy interval of the protons are folded in.

The monotonic contribution comes from the 3 body neutral decays:



In the following paragraph we evaluate the branching ratio R between the $\gamma + \gamma$ decay and the $3\pi^0$ plus $\pi^0 + \gamma + \gamma$ decays, on the basis of the distributions we have presented in fig. 6, 7 and 9, 10, 11 upper part. That is, we will evaluate the quantity

$$(7) \quad R = \frac{\Gamma(\gamma + \gamma)}{\Gamma[(3\pi^0) + (\pi^0 + \gamma + \gamma)]}$$

in four different ways.

The ratio R given in (7) shall be compared with the ratio $\Gamma(\gamma + \gamma) / \Gamma(3\pi^0)$ of other experiments (see Section 4). In fact in no experiment the $\pi^0 + \gamma + \gamma$ decay could be until now separated by the $3\pi^0$ decay. Contrarily at least apparently to other authors, we do not think that there is until now any precise argument to consider the $\pi^0 + \gamma + \gamma$ decay very small.

Section 4 - EVALUATION OF THE BRANCHING RATIO R BETWEEN THE $\gamma + \gamma$ DECAY MODE AND OTHER NEUTRAL MODES. -

In order to get the value of R, both from the results of the step method and of the γ -method, the following informations are needed:

a) The efficiencies of detection of our apparatus for the three considered decays: $\gamma + \gamma$; $3\pi^0$; $\pi^0 + \gamma + \gamma$.

b) The fraction of observed events which can be attributed to each possible decay (in practice, $\pi^0 + \gamma + \gamma$ can not be separated by $3\pi^0$).

We give now some details about points a) and b).

a) The efficiencies of detection.

No hypothesis is needed to evaluate the geometrical efficiency ε_γ of detection of the mode $\eta \rightarrow \gamma + \gamma$. In fact this is a two body decay which is isotropic in the rest system of the η . A simple Lorentz transformation of the solid angle of the Cerenkov C (see fig. 1) to the rest frame system of the η then gives:

$$\varepsilon_\gamma = \frac{(1 + \beta)(1 - \cos \theta)}{1 - \beta \cos \theta}$$

where β is the velocity of the η (in units c) and θ is the angular aperture of the Cerenkov counter. For each kinematical situation, β is a constant.

On the contrary, to evaluate the efficiency of detection of the modes $\eta \rightarrow 3\pi^0$ and $\eta \rightarrow \pi^0 + \gamma + \gamma$ the knowledge of the γ -spectra from these decays is needed. As we have seen (Section 2) those spectra have been calculated under reasonable hypothesis (spectra ϕ_2 and ϕ_3 of fig. 5). Once ϕ_2 and ϕ_3 are known, the efficiencies are easily evaluated:

$$\varepsilon_{3\pi^0} = \frac{3(1 + \beta)(1 - \cos \theta)}{1 - \beta \cos \theta} \frac{\int_{E_1}^{E_2} \phi_2(E_\gamma) dE_\gamma}{\int_0^\infty \phi_2(E_\gamma) dE_\gamma}$$

$$\varepsilon_{\pi^0\gamma\gamma} = \frac{2(1 + \beta)(1 - \cos \theta)}{1 - \beta \cos \theta} \frac{\int_{E_1}^{E_2} \phi_3(E_\gamma) dE_\gamma}{\int_0^\infty \phi_3(E_\gamma) dE_\gamma}$$

E_1 and E_2 are the minimum and maximum energy cut-offs for the γ rays accepted by C. (For instance in the step measurements $E_1 = 240$ MeV, $E_2 = 400$ MeV).

It is important to note that the quantities $\varepsilon_{\gamma\gamma} / \varepsilon_{3\pi^0}$, $\varepsilon_{\gamma\gamma} / \varepsilon_{\pi^0\gamma\gamma}$ which are needed for the evaluation of the branching ratio R are independent of the geometry, since θ (aperture angle of the Cerenkov) does not appear in it.

In the γ -method, where we have used $E_1 = 270$ MeV, $E_2 = \infty$, the efficiencies of detection of the $\eta \rightarrow \gamma + \gamma$, $\eta \rightarrow 3\pi^0$, $\eta \rightarrow \pi^0 + \gamma + \gamma$ modes, were

$$(8) \quad \varepsilon_{\gamma\gamma} = 10\% ; \quad \varepsilon_{3\pi^0} = 10.6\% ; \quad \varepsilon_{\pi^0\gamma\gamma} = 11.2\% .$$

Possible sources of errors in the evaluation of the efficiencies are discussed in Appendix 1.

The values (8) indicate that the efficiencies $\varepsilon_{3\pi^0}$ and $\varepsilon_{\pi^0\gamma\gamma}$ are the same, at least in the γ method (in the step method the situation is

somewhat different, due to the different cuts in the γ spectrum).

We must make a few remarks on the $\pi^0\gamma\gamma$ decay mode. In fact (see § 7 where we discuss our results) if we stick to the model of Gell-Mann and cow. (22), the $\pi^0+\gamma+\gamma$ decay mode should be rather improbable, and R is mostly the ratio between the $\gamma+\gamma$ and the $3\pi^0$ decay mode. This is the trend actually taken (for good reasons or not) by many authors^(15,23). Considering that the $\pi^0+\gamma+\gamma$ mode is not forbidden by any obvious selection rule we prefer to carry out our discussion without disregarding the possible presence of this decay mode.

This possibility is allowed by the important fact that the efficiency of our apparatus for detecting a $3\pi^0$ and a $\pi^0+\gamma+\gamma$ decay is the same, when the γ method is used, within an approximation smaller than our statistical errors.

We must remind that in all the published experiments the $\pi^0+\gamma+\gamma$ decay could not be distinguished by $3\pi^0$, and in all the experiments the widths or branching ratios referring to $3\pi^0$ should refer to $3\pi^0$ and $\pi^0+\gamma+\gamma$ in still unknown mixtures.

b) Separation and determination of the events due to the different decay modes.

Let us consider first the γ method for which $\varepsilon_{3\pi^0} \simeq \varepsilon_{\pi^0\gamma\gamma}$.

For the γ -method, the following procedure was used; the η -events (figg. 9, 10 and 11 upper part) have been fitted with curves of the type:

$$a\phi_1 + b\phi_2$$

The least square best fit values of a and b are proportional to the contribution of the $\gamma+\gamma$ and $3\pi^0$ events, if the $3\pi^0$ is the only neutral decay in more than two bodies. Since the efficiency of detection of the $3\pi^0$ and $\pi^0+\gamma+\gamma$ decay modes are the same, the value of R we get in this way represents the ratio $\Gamma(\gamma\gamma)/\Gamma(3\pi^0)$ if the $\pi^0+\gamma+\gamma$ mode is not there, or the ratio $\Gamma(\gamma\gamma)/\Gamma[(3\pi^0)+(\pi^0\gamma\gamma)]$ if the decay $\eta \rightarrow \pi^0+\gamma+\gamma$ is present.

It is worth noticing the following points: the confidence level of the χ^2 test obtained by a fit with a curve $a\phi_1 + b\phi_2$ is always rather good (25%, 50%, 75%). Only a small improvement ($\simeq 10\%$) is obtained by fitting the η events with a curve $a\phi_1 + b\phi_2 + c\phi_3$ while a fit of the type $a\phi_1 + b\phi_3$ is rather poor (confidence level of the χ^2 test $\sim < 1\%$).

This could be an indication that the $\eta \rightarrow 3\pi^0$ mode is the main multi-body neutral decay of the η .

For the step method, an insight to fig. 5 allows the following conclusions:

For $E_\gamma < 400$ MeV, the η events (fig. 7b) are essentially due to the decays $\eta \rightarrow 3\pi^0$ and $\eta \rightarrow \pi^0+\gamma+\gamma$. For $E_\gamma > 400$ (fig. 6b), the events are due to the $\gamma+\gamma$ decay mode, plus a known percentage of the events $\eta \rightarrow 3\pi^0$ and $\eta \rightarrow \pi^0+\gamma+\gamma$.

The knowledge of the number of events of figg. 6b and 7b, and of the efficiencies of detection of the decays $\eta \rightarrow \gamma + \gamma$, $\eta \rightarrow 3\pi^0$ and $\eta \rightarrow \pi^0 + \gamma + \gamma$ as a function of the cut-off energies on C, allow therefore the calculation of R.

To do this a last correction must be applied, to take into account the contribution of the $\pi^+ + \pi^- + \pi^0$ and $\pi^+ + \pi^- + \gamma$ decays to our events, and therefore, the value of the ratios

$$A = \frac{\Gamma(\text{neutrals})}{\Gamma(\pi^+ \pi^- \pi^0)} \quad \text{and} \quad B = \frac{\Gamma(\text{neutrals})}{\Gamma(\pi^+ \pi^- \gamma)} \quad \text{is needed.}$$

We have used the value $A = 2.5 \pm 0.4$ (1, 2, 8, 9). The error in A does not affect appreciably the value of R, since the overall correction is $\sim 15\%$. The correction due to the presence of the $\pi^+ + \pi^- + \gamma$ mode is negligible.

At the end the value of R in the \mathcal{J} -method is

$$(9) \quad R = \frac{3A + 1}{3(b/a \cdot \frac{\mathcal{E}_{\mathcal{J}\mathcal{J}}}{\mathcal{E}_{3\pi^0}}) \cdot A - 1}$$

In practice, our statistics and our errors do not allow what in principle could be possible: to compare the \mathcal{J} -method and the step method to separate the possible $\pi^0 + \gamma + \gamma$ contribute from the $3\pi^0$. All what we can get is a guess: that the $\pi^0 + \gamma + \gamma$ mode, considering the coherence of our results and the indication of the best fits, is probably smaller than the $3\pi^0$ mode. In the calculation of R in the step method we assumed the efficiency $\mathcal{E}_{3\pi^0}$ corresponding to the hypothesis that the $\pi^0 + \gamma + \gamma$ mode may be disregarded. This should not introduce any sensible error.

All the experimental values of R we obtained with the two methods are reported in Table I.

Due to the nature of our method, it is not valid to assume that the errors are purely statistical. Possible systematic errors might have entered in the elimination of the multipion background, and in the evaluation of the efficiency of the Cerenkov counter (see Appendix 1). Those errors have been estimated, and they have been included in the errors quoted in Tab. I.

The values of R given in the third and the fourth row are in parenthesis: in fact we believe that these values are less certain, due to some possible larger systematic errors: in these cases the spark chamber works as an anticoincidence, and we do not see the proton track; furthermore we need a larger extrapolation in the evaluation of the multipion background.

The weighted average of the two measurements of R, not in parenthesis in Table I gives the value

$$(10) \quad R = .8 \pm .25$$

The values of R reported here are the same as recently published in a preliminary note⁽¹⁶⁾.

TABLE I

E_0 (MeV)	$K^\pm \Delta K$ (MeV)	$T_p^\pm \Delta T_p$ (MeV)	R	Method	Dose (10^{14} equiv. quanta)
1000	978 ± 22	278 ± 18	0.78 ± 0.34	γ -method	2.05
1000	978 ± 22	278 ± 18	0.83 ± 0.31	step	3.5
1000	939 ± 14	248 ± 11	(0.53 ± 0.22)	γ -method	1.53
950	937 ± 13	247 ± 10	(0.88 ± 0.58)	γ -method	1.95

Results of the present experiment (reaction $\gamma + p \rightarrow \eta + p$). E_0 is the energy of the electrons in the synchrotron; $K^\pm \Delta K$ is the lab. energy and energy interval of the photons producing the reaction $\gamma + p \rightarrow \eta + p$ with θ recoil proton of energy $T_p^\pm \Delta T_p$ entering the proton channel; $R = [\Gamma(\gamma\gamma)] / [\Gamma[(3\pi^0) + (\pi^0\gamma\gamma)]]$ is the branching ratio defined in § 4. The numbers in parenthesis are less certain: see text. The errors include an estimate of our uncertainties in efficiency, background and accidentals.

TABLE II^(x)

Percentages of the various decay modes of the η , in the assumption that other possible decay modes not listed in the table are irrelevant.

$\eta \rightarrow \gamma\gamma$: 31.5 ± 5.5 %
$\eta \rightarrow 3\pi^0 + \pi^0\gamma\gamma$: 35.0 ± 6.2 %
$\eta \rightarrow \pi^+\pi^-\pi^0$: 26.6 ± 2.8 %
$\eta \rightarrow \pi^+\pi^-\gamma$: 6.9 ± 2.1 %

The errors are obtained by propagation of the errors given by each author.

(x) - This table does not agree with a set of values given by S. Okubo and B. Sakita⁽²⁴⁾. We could not find in the literature the origin of some results of surprising precision, such as $\Gamma(\gamma\gamma) / \Gamma(\pi^+\pi^-\pi^0) = 1.9 \pm 0.13$.

TABLE III

E_0 (MeV)	$K^\pm \Delta K$ (MeV)	$T_p^\pm \Delta T_p$ (MeV)	$\theta^{* \pm} \Delta \theta^{*}$	$\frac{(d\sigma/d\Omega^*)}{(\Gamma_{\gamma\gamma}/\Gamma_{\text{tot}})}$ (10^{-32} cm ² /st)	$(d\sigma/d\Omega^*)$ 10 ⁻³² cm ² /st	Method	Dose (10^{14} e. q.)
1000	978 ± 22	278 ± 18	$106^{0 \pm 5^0}$	7.6 ± 1.6	~ 24	γ -method	2.05
1000	978 ± 22	278 ± 18	$106^{0 \pm 5^0}$	6.2 ± 1.3	~ 20	step	3.5
1000	939 ± 14	248 ± 11	$103^{0 \pm 5^0}$	(11.5 ± 2.6)	(~ 36)	γ -method	1.53
950	937 ± 13	248 ± 11	$103^{0 \pm 5^0}$	(10 ± 2.1)	(~ 32)	γ -method	1.95

Values of the diff. cross section in the c. m. for the reaction $\gamma + p \rightarrow \eta + p$, E_0 , $K^\pm \Delta K$ and $T_p^\pm \Delta T_p$ as in Table I, $\theta^{* \pm} \Delta \theta^{*}$ is the c. m. angle and the angle interval of the η ; $(d\sigma/d\Omega^*) / (\Gamma_{\gamma\gamma} / \Gamma_{\text{total}})$ is the differential cross section in the c. m. for photoproduction of the η decaying in the $\gamma + \gamma$ mode (this is in fact one of the values which we can directly obtain from our experiment); $d\sigma/d\Omega^*$ is the c. m. differential cross section for η photoproduction (3.2 times the preceding values, as obtained from Table II).

In making a further critical analysis of the results we find two possible sources of systematic errors:

a) The multipion background in the region of the η may have a distribution somewhat different than equations (4), (5), (6). In particular the hypothesis b) of § 2, that is the assumption that the contribution of protons in the photon energy interval $\Delta E_\gamma = 950-1000$ MeV is practically flat, is valid in the case of double production (reaction (3a)), not in the case of reaction (3b). A preliminary phase space exploration indicates in the case of three pion production a rather steep decrease of N versus T_p , rather than a flat behaviour. Having disregarded the 3-pion contribution has the tendency to lower the value of R.

b) We have not measured precisely enough the contribution of the accidentals, and probably, as indicated by further verifications, the accidental correction is smaller than the corrections introduced by us. This overestimate has in our case the tendency to increase the value of R, so that the two systematic errors a) and b) go in opposite directions.

All these points will be clarified in the new experiment we are starting. Anyway we do not expect that all these possible effects may change appreciably our results on R, as given in Table I.

The value may be compared with recent experimental results of other authors:

$$(11) \quad \text{Crawford et al. (15)} \quad R = 1.5 \pm 0.9$$

$$(12) \quad \text{A. Muller et al. (23)} \quad R = 1.1 \pm 0.5$$

M. Chretien et al. (13) have a lower limit: $R \geq 0.9 \pm .25$.

Section 5 - LIST OF THE PERCENTAGES OF THE DECAY MODES OF THE η .

Using the experimental information published up to now, it is possible to get, still with large errors, a list of the percentages of the various decay modes of the η .

The pieces of information we use are the following

$$R = \frac{\Gamma(\gamma\gamma)}{\Gamma[(3\pi^0) + (\pi^0\gamma\gamma)]} ; \quad A = \frac{\Gamma(\text{all neutrals})}{\Gamma(\pi^+\pi^-\pi^0)} ; \quad B = \frac{\Gamma(\pi^+\pi^-\gamma)}{\Gamma(\pi^+\pi^-\pi^0)}$$

The weighted average of the values (10), (11), (12) gives

$$(13) \quad R = 0.9 \pm 0.22$$

The result of Chretien et al. (13) has not been included in the average, since it is a lower limit; anyway it agrees with (13) very well. In all the experiments used for the average, distinction between the decays $\eta \rightarrow 3\pi^0$ and $\eta \rightarrow \pi^0 + \gamma + \gamma$ could not be done. We continue therefore to keep together these two neutral decay modes without assuming that the decay $\eta \rightarrow \pi^0 + \gamma + \gamma$ is irrelevant.

The ratio A has also been measured by different authors. M. Meer et al. (5) give

$$A = 3.1 \pm 1.2$$

Alff et al. (8) give for the ratio $\Gamma(\text{neutrals})/\Gamma(\text{charged}) = 2.5 \pm 0.5$. Since their events $\eta \rightarrow (\text{charged})$ are fitted by a $\pi^+ + \pi^- + \pi^0$ system, the value they quote is to be interpreted as $A = 2.5 \pm 0.5$. Crawford et al. (15) give $\Gamma(\text{neutrals})/\Gamma[(\pi^+ \pi^- \pi^0) + (\pi^+ \pi^- \gamma)] = 1.65 \pm 0.53$. Using this figure and the value of B measured by Fowler et al. (9) we get $A = 2.1 \pm 0.7$. By average over the values we have

$$A = 2.5 \pm 0.4$$

Finally, B has been measured by Fowler et al. (9)

$$B = 0.26 \pm 0.08$$

Using the average values of R, A, B we obtain for the η decays the percentages given in Table II.

Section 6 - A FIRST ESTIMATE OF THE CROSS SECTION FOR THE PROCESS $\gamma + p \rightarrow \eta + p$ -

Further work is being devoted to the important question of the value of the cross section for process (1). We only report in Table III the results of a first estimate of the differential cross section at some energies of the primary photon, at an angle $\sim 100^\circ$ of the η in the c. m.

Specifically, the partial cross section in the c. m. system is given in our experiment by

$$\frac{d\sigma}{d\Omega^*} \frac{\Gamma(\gamma\gamma)}{\Gamma(\text{all modes})} = \frac{m(\theta)}{nN \varepsilon_1 \varepsilon_2 \varepsilon_{\gamma\gamma} \Delta\Omega} \frac{d\Omega}{d\Omega^*}$$

where:

- $m(\theta)$ is the number of η events observed;
- $n = 3 \times 10^{23} = DN_A l$ is the number of protons per square centimeter in the Hydrogen target (D, density of H_2 0.07 g/cm³; N_A Avogadro number; $l = 7$ cm, is the length of our target;
- $N = (\Delta K/K)Q$ is the number of photons in the interval ΔK when Q equivalent quanta are measured on the quantameter⁽¹⁷⁾;
- $\varepsilon_1 = 0.50$ is the efficiency of detection of the protons in the proton channel (it takes into account Coulomb scattering and nuclear interactions losses);
- $\varepsilon_2 = 0.88$ is the efficiency of detection of the γ 's which are emitted in the directions of the Cerenkov (it takes into account the γ -rays lost for conversion in the wood shielding);
- $\varepsilon_{\gamma\gamma}$ is the geometrical efficiency of the Cerenkov for γ rays from the process $\eta \rightarrow \gamma + \gamma$ (see Section 4);
- $\Delta\Omega$ is the lab. solid angle of the proton telescope. Its value for the protons detected in the S. C. is 2.2×10^{-3} sr. The value of $\Delta\Omega$ is more uncertain in the measurement in parenthesis in Table III;
- $d\Omega/d\Omega^* = 7.6$ is the transformation factor of the solid angle from laboratory to c. m. system.

Our results are not in contradiction with a previous attempt to observe the photoproduction of the η .

In fact Berkelman and cow.⁽²⁵⁾, looking at reaction (1) could give an upper limit of about $0.5 \mu\text{b}/\text{sr}$ for the photoproduction of a particle of mass 550 MeV.

More recently, B. Delcourt et al.⁽²⁶⁾ have done a measurement of the differential cross section for η photoproduction near the threshold; their results seem to indicate that the η is photoproduced near the threshold with a cross section greater than that of our present experiment.

Section 7 - DISCUSSION OF THE RESULTS. COMPARISON WITH THEORY. -

The results on the branching ratio we have given in Table II can be compared with the available theoretical predictions. Several different theoretical models have been proposed in connection with the various decay modes of the η . A first theoretical approach to the problems above mentioned is due to Gell-Mann, Sharp and Wagner⁽²²⁾ who suggested that the radiative decays of the η could be explained through a limited number of basic quantities; the $\rho\pi\pi$ coupling, the $\omega\rho\pi$ coupling, the direct $\rho\rho$ and $\rho\omega$ couplings, and finally the couplings $\eta\rho\rho$ and $\eta\omega\omega$.

The radiative decays $\eta \rightarrow 2\gamma$ and $\eta \rightarrow \pi^+\pi^-\gamma$ would proceed predominantly by a primary strong dissociation into two virtual vector particles, which could be ρ 's. Therefore the intermediate steps would be $\eta \rightarrow 2\rho$, both ρ 's $\rightarrow \gamma$ for the $\eta \rightarrow 2\gamma$ decay, and one $\rho \rightarrow \gamma$ and the other $\rho \rightarrow \pi^+\pi^-$ for the $\eta \rightarrow \pi^+\pi^-\gamma$ decay. (see the diagrams a) and b) in fig. 12).

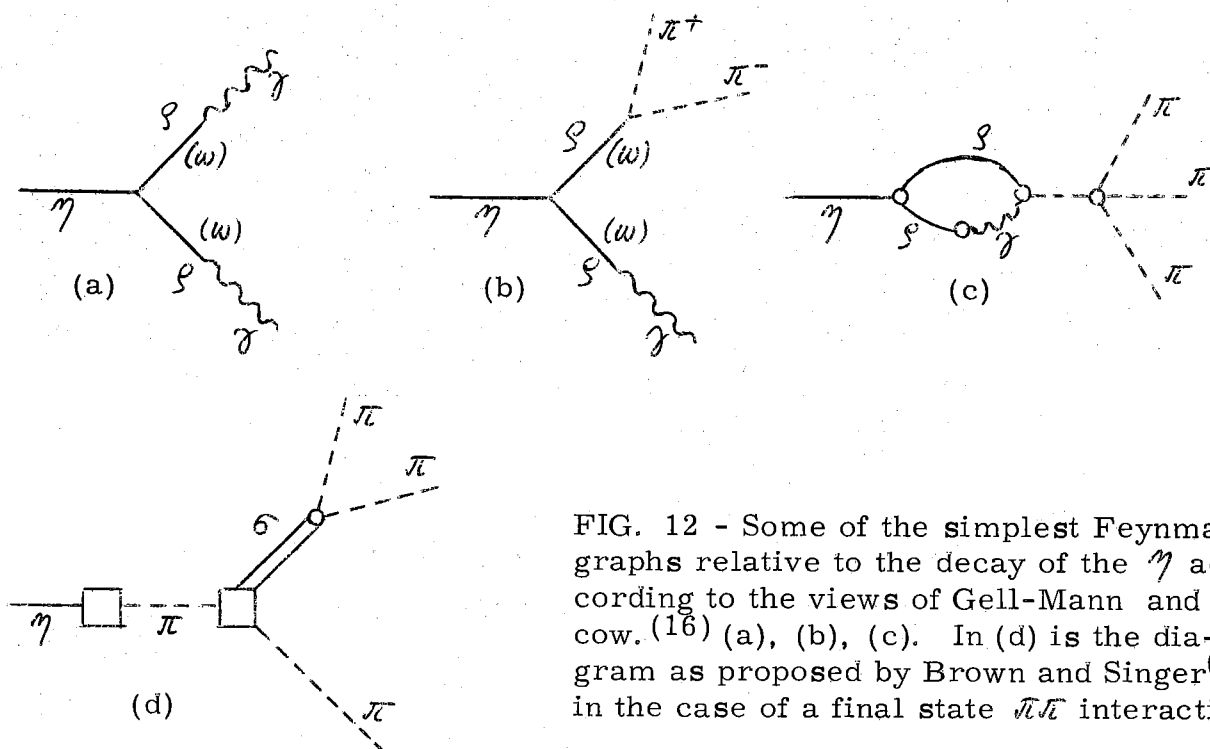


FIG. 12 - Some of the simplest Feynman graphs relative to the decay of the η according to the views of Gell-Mann and cow.⁽¹⁶⁾ (a), (b), (c). In (d) is the diagram as proposed by Brown and Singer⁽¹⁸⁾ in the case of a final state $\pi\pi$ interaction.

Following this scheme it is found:

$$(14) \quad \frac{\Gamma_{\eta}(\pi^+\pi^-\gamma)}{\Gamma_{\eta}(\gamma\gamma)} \simeq \frac{1}{2} \left(\frac{\mathcal{G}_{3\pi\pi}^2}{4\pi} \right) \left(\frac{\mathcal{G}_5^2}{4\pi} \right).$$

The effect of the inclusion of $\eta \rightarrow 2\omega \rightarrow 2\gamma$ can be estimated when, according to the unitary symmetry, it is assumed $\eta\omega\omega = -\eta\omega\omega$ (22, 27, 28). In this case a factor 9/4 must be applied to (14), so that, taking as a crude estimate⁽²²⁾ $(\mathcal{G}_{3\pi\pi}^2/4\pi) \simeq (\mathcal{G}_5^2/4\pi) \simeq 1/2$ the expected value of the branching ratio (A) becomes

$$\Gamma_{\eta}(\pi^+\pi^-\gamma)/\Gamma_{\eta}(\gamma\gamma) \simeq 0.12 \times 9/4 \simeq 0.25^{(29)}.$$

This value may be compared with the experimental ratio obtained by the Table II: 0.22 ± 0.08 . If we stick to the model of Gell-Mann et al.⁽²²⁾ the $\pi^0 + \gamma + \gamma$ decay mode should be rather improbable, as estimated by Ferrari and Holloway⁽²⁸⁾, who find $\Gamma(\pi^0\gamma\gamma)/\Gamma(\gamma\gamma) \simeq 10^{-5}$. There is till now no experimental evidence for this decay, which we reconsider in the following.

As far as the connection between the radiative decays and the pionic ones is concerned, the Gell-Mann et al.⁽²²⁾ scheme is not so immediate. For instance, one of the simplest diagrams for the 3π modes is shown in fig. 12c. According to Barton and Rosen⁽³⁰⁾, this model makes it impossible to form a reliable estimate of the ratio of the 3π to the other modes. Furthermore other general remarks have been done^(31, 32); the point is that in the Gell-Mann calculations it has been completely neglected the large structure effects in the π^0 decay form factor, which now seem quite well established experimentally.

A single pion intermediate state like at the right of fig. 12c) has been also suggested⁽³³⁾ to explain the $K \rightarrow 3\pi$ (τ and τ') decays. It must be noted, in fact, that every model of η -decay has implications for K-meson decays to three pions; thus additional tests can be made of the theory. Then the η , τ and τ' decay amplitudes can be interpreted as just different isotopic projections of the same function, apart from a constant factor depending on the mechanism whereby the single-pion state is reached, which will be different for K and η : in the case of the η , the $\eta \rightarrow \pi$ goes through an α^2 "black box"; in the case of the K, the $K \rightarrow \pi$ goes through a weak coupling. As a consequence, once the single-pion intermediate state has interceded, the Dalitz plots for η and K decay into three pions should be determined by the $\pi \rightarrow 3\pi$ amplitude, so that the π^0 kinetic energy spectrum in $\eta \rightarrow \pi^+ + \pi^- + \pi^0$ would be very similar to the π^+ spectrum of $\tau'^+ \rightarrow \pi^+ + \pi^+ + \pi^-$ decay.

The similarity in the Dalitz plots of $\eta \rightarrow \pi^+ + \pi^- + \pi^0$ and $\tau'^+ \rightarrow \pi^+ + \pi^+ + \pi^-$ is a quite well established experimental fact^(34, 35).

It has been pointed out, however, by Bég⁽³⁶⁾ and, independently, Wali⁽³⁷⁾ and summarized by Kacser⁽³⁸⁾ that such agreement is not necessarily due to the predominant pion pole model in K decay, but is already a consequence of the assigned quantum numbers (0^{-+}) for the η together with a pure I=1 final state for K decay. Furthermore, Wali⁽³⁷⁾ pointed out that the $3\pi^0$ to $\pi^+ + \pi^- + \pi^0$ branching ratio of the η is uniquely related to the π^0 energy spectrum in the decay $\eta \rightarrow \pi^+ + \pi^- + \pi^0$. Thus, from the analysis of the

$\eta \rightarrow 3\pi$ and $K \rightarrow 3\pi$ Dalitz plots he could give a prevision for the ratio $\Gamma(3\pi^0)/\Gamma(\pi^+\pi^-\pi^0)$. When the mass corrections are considered, this ratio is of the order of 1.6 - 1.7.

The experimental value $\Gamma_\eta(3\pi^0)/\Gamma_\eta(\pi^+\pi^-\pi^0)$ is actually (see Table II) $\leq 1.32 \pm 0.27$, where the equality holds if we assume that the $\pi^0 + \gamma + \gamma$ mode is negligible. The value of the $\Gamma(3\pi^0)/\Gamma(\pi^+\pi^-\pi^0)$ ratio depends on the $\pi\pi$ interaction in the final state. A detailed investigation of the consequences of a strongly attractive energy dependent S-wave two pion interaction in the I=0 state has been done by Brown and Singer^(27,35). They represent phenomenologically this two-pion interaction (see fig. 12d) as a dipion "particle" σ having a finite width, and they find a good agreement with the η Dalitz plot when one assumes $m_\sigma \approx 400$ MeV, $\Gamma_\sigma = 75 - 100$ MeV.

More recently, following the same lines, Crawford et al.⁽³⁹⁾, have done an accurate analysis on a selected set of 96 η 's quite free from background; they find $m_\sigma = 381 \pm 5$, $\Gamma_\sigma = 48 \pm 8$ MeV. The decay mechanism through the σ leads naturally to an enhancement of the $\eta \rightarrow \pi^+\pi^-\pi^0$ relative to the $\eta \rightarrow 3\pi^0$ mode; the value found by Brown and Singer⁽³⁵⁾ is

$$\Gamma_\eta(3\pi^0)/\Gamma_\eta(\pi^+\pi^-\pi^0) \simeq 1.35$$

which is in good agreement with the quoted experimental value 1.32 ± 0.27 .

The existence of a σ particle like in the Brown and Singer model can enhance the $\eta \rightarrow 3\pi$ mode relative to the radiative modes. It is worth noticing that the $\eta \rightarrow \pi^+\pi^-\gamma$ is not enhanced as $\eta \rightarrow \sigma + \gamma$ is strongly forbidden by charge conjugation invariance.

An estimate of $\eta \rightarrow \pi^+\pi^-\pi^0$ width done⁽³⁵⁾ on these lines gives a value: $\Gamma_\eta(\pi^+\pi^-\pi^0) \approx 200$ eV. Following the ρ, ω model of Gell-Mann et al.⁽²²⁾, Brown and Singer, in a previous paper⁽²⁷⁾, found the absolute values: $\Gamma(\gamma\gamma) \approx 160$ eV, $\Gamma(\pi^+\pi^-\gamma) \approx 20$ eV so that, combining these results, the following theoretical predictions are reached:

$$\Gamma(\gamma\gamma)/\Gamma(\pi^+\pi^-\pi^0) \approx 160/200 \approx 0.8$$

to be compared with the measured value (see Table II): 1.18 ± 0.24 and $\Gamma(\pi^+\pi^-\gamma)/\Gamma(\pi^+\pi^-\pi^0) \approx 20/200 = 0.1$ to be compared with the measured value⁽⁹⁾ 0.26 ± 0.08 . Another recent qualitative attempt to give some predictions on the partial widths for the η decays is due to Riazuddin and Fayyazuddin⁽⁴⁰⁾. They calculate the partial widths for the $\pi^+\pi^-\pi^0$ and $3\pi^0$ modes via an effective electromagnetic vertex $\eta \rightarrow \pi^0$, the strength of which influences the nucleon-nucleon interaction.

A rather different theoretical approach is the following. Barrett and Barton⁽⁴¹⁾ start from the relations of the unitary symmetry realized in the eightfold way and the rules for calculating electromagnetic interactions, established by Cabibbo and Gatto⁽⁴²⁾.

In this case the η is considered the isosinglet member of pseudo-scalar octet ($\bar{\pi}\eta\bar{K}\bar{K}$) and the amplitudes of the decays $\pi^0 \rightarrow 2\gamma$ and $\eta \rightarrow 2\gamma$ are simply related:

$$M(\eta \rightarrow 2\gamma) = \frac{1}{\sqrt{3}} M(\pi^0 \rightarrow 2\gamma).$$

From this relation and using the known value of the π^0 meanlife they obtain $\Gamma(\gamma\gamma) \simeq 60 - 170$ eV. As far as the decay $\eta \rightarrow \pi^+ + \pi^- + \pi^0$ is concerned, they assume the virtual sequence $\eta \rightarrow \pi^0 \rightarrow \pi^+ + \pi^- + \pi^0$ so that the amplitude is

$$M(\eta \rightarrow \pi^+ + \pi^- + \pi^0) = r \lambda / (m_\eta^2 - m_{\pi^0}^2)$$

λ being the $\pi\pi$ coupling constant, and r the contribution of $\eta - \pi^0$ black box. The value of r is still calculated by the formulae of Cabibbo and Gatto⁽⁴²⁾ and the width $\Gamma(\pi^+ \pi^- \pi^0) \approx 110$ eV is obtained.

The branching ratio $\Gamma(\gamma\gamma)/\Gamma(\pi^+ \pi^- \pi^0)$ is in qualitative agreement with the experiment; in fact (see Table II and Table IV, where we give in synthesis a comparison of the theory and the experiments) the experimental value is 1.8 ± 0.24 . An attempt to obtain results in agreement with the experiment has been made by Susumo Okubo and Bunji Sakita⁽²⁴⁾, who make use of a lot of theoretical arguments, according to which the $\pi^+ \pi^- \gamma$ mode becomes rather important and what is worth noticing, the $\pi^0 + \gamma + \gamma$ mode becomes relatively relevant.

The $\pi^0 + \gamma + \gamma$ mode is very difficult to be observed, and we already said that it is expected to be small in all the models reported above.

This "forgotten" decay mode may appreciably contribute to the width of the η and, moreover, it can discriminate among different theories, if one accepts the recent suggestion by Bronzan and Low⁽⁴³⁾. These authors propose a new selection rule for bosons, whose violation occurs with about the same frequency as single photon emission ($\approx 1\%$). According to this rule $\eta \rightarrow \pi^+ + \pi^- + \gamma$ and $\eta \rightarrow 2\gamma$ are forbidden, and $\eta \rightarrow \pi^0 + \gamma + \gamma$ as well as $\eta \rightarrow 3\pi$ are allowed: this could adjust the puzzling question of the abundance of the 3π decays relative to the radiative ones.

On the basis of these results it is convenient to continue to keep together the $\eta \rightarrow 3\pi^0$ and $\eta \rightarrow \pi^0 + \gamma + \gamma$ possibilities in all the experiments where these two modes cannot be separated, that is in all the present experiments.

A verification of the existence or the upper limit of the $\pi^0 + \gamma + \gamma$ mode has become now highly desirable. From the partial account of the theoretical approaches till now available and the comparison of the experimental results with the theoretical predictions we reported above (see also the synthesis in Table IV), it appears reasonable to make the following remarks.

The theory is still far from giving a clear and unique picture of the η decays, mostly due to the fact that the electromagnetic order in α and the phase space considerations lead to irreconcilable consequences, unless one makes use of "ad hoc" arguments like, for instance, new selection rules.

On the experimental side we remark that the theoretical speculations are still much too free due to the lack of at least the following experimental informations:

- a) a more precise determination of the branching ratio ($\eta \rightarrow$ neutrals)/($\eta \rightarrow$ charged);
- b) an answer to the existence or not of the $\pi^0 + \gamma + \gamma$ decay mode;
- c) an absolute measurement (at least order of magnitude) of the total width of the η .

TABLE IV

Relative and total widths of the η . A comparison between the experimental situation and the theoretical predictions (see § 7). By $\Gamma(\pi^+\pi^-\gamma)$ we mean the width of the $\eta \rightarrow \pi^+\pi^-\gamma$, similarly for the other widths.

Widths relative and total	Experimental value	Theoretical value	Basis of theoretical calculations	Authors
$\frac{\Gamma(\pi^+\pi^-\gamma)}{\Gamma(\gamma\gamma)}$	0.26 ± 0.08 (9)	~ 0.25 ~ 0.07	Decay through two virtual vector mesons + unitary symmetry Idem	Gell-Mann et al. (22) Brown et al. (27, 35) Ferrari et al. (28)
$\frac{\Gamma(\pi^0\pi^0\pi^0)}{\Gamma(\pi^+\pi^-\pi^0)}$	1.32 ± 0.27 (see table II)	≤ 1.7 $1.6 \rightarrow 1.7$ 1.35	Similarity of the final states for K and η decays into 3π " " " " " " " " " " " " + strong $\pi\pi$ I = 0, S-wave final state interaction	Feinberg et al. (36) Wali (37) Brown et al. (27, 35)
$\frac{\Gamma(\gamma\gamma)}{\Gamma(\pi^0\pi^0\pi^0)}$	0.9 ± 0.22 (see sect. 5)	$0.4 \rightarrow 1.2$ $\sim .7$ $\sim .55$	Unitary symmetry model Unitary symmetry model	Barrett et al. (41) Cabibbo et al. (42) Okubo et al. (24) Brown et al. (35)
$\frac{\Gamma(\pi^0\gamma\gamma)}{\Gamma(\text{all modes})}$?	$\approx 10^{-5}$ a few %	Decay through two virtual vector mesons + unitary symmetry Use of the $\eta\pi^0\gamma\gamma$ boson vertex	Ferrari et al. (28) Okubo et al. (24)
Γ (all modes)	≈ 10 MeV	~ 650 eV ~ 600 eV ~ 400 eV ~ 80 eV	Influence of $\eta\pi^0$ vertex of the nucleon-nucleon interaction	Brown et al. (35) Okubo et al. (24) Barrett et al. (41) Riazzudin et al. (40)

Appendix 1 - SOURCES OF ERRORS. -

In an experiment with low counting rate and high background particular care must be used in order to avoid systematical errors. In the following possible sources of errors are listed and discussed.

Accidental and empty target rate. -

The accidental rate was systematically measured (and subtracted) by delaying counters of an amount $n\tau$, an integer multiple of the time-distance among two R. F. bunches of the synchrotron. Most of the rate is due to an accidental coincidences between protons and γ -rays in the Cerenkov C. For the accidental counts of this type, the γ spectrum in C and the proton spectrum in the spark chamber could be determined with good statistics, by measuring the γ spectrum of random pulses in C during the machine-time, and by triggering the spark chamber with protons without the request of being a coincidence with a γ -ray. Empty target background was also measured and subtracted. Both these type of background do not appreciably contaminate the $\eta \rightarrow \gamma + \gamma$ measurements. The contamination in the $\eta \rightarrow 3\pi^0$ region was sometimes as high as 30%.

Spark chamber efficiency. -

The spark chamber efficiency per gap was systematically checked to be higher than 98%. Possible jitter in time of the spark gap could cause random inefficiency and the loss of good tracks. For this reason the time of the spark gap was systematically checked during the runs. In addition the spark chamber was sometimes put in the middle of the proton telescope: 100% of the photos contain in this case a good track. No correction was thus applied for this effect.

Energy calibration of the Cerenkov. -

The energy calibration of the Cerenkov must not change during the runs. A change in the calibration could smearing the peak due to the η . In addition the efficiency of detection of the process $\eta \rightarrow 3\pi^0$ and $\eta \rightarrow \pi^0 + \gamma + \gamma$ depend on the energy calibration. For this reason the calibration of the Cerenkov was checked every few hours by means of cosmic-rays spectra. The absolute calibration was made before, during and after the measurement with monochromatic electrons. A possible error in the energy calibration was however considered in the evaluation of the efficiency of detection of $\eta \rightarrow 3\pi^0$ and $\eta \rightarrow \pi^0 + \gamma + \gamma$ and propagated to the branching ratio ($\sim 20\%$ effect).

Solid angle determination. -

The solid angle determination can be affected by errors due to counter alignment, counter efficiency, coulomb and diffraction scattering etc.

For the spark chamber measurements the solid angle can be determined with some care by making a distribution of the events as a function of the entrance point in the chamber. A correction was thus applied using this experimental information to correct for losses at the edges. The solid angle for the counter measurements is more uncertain (rows 3, 4, 5 and 6 of Table I). The corresponding cross section may contain some systematical error

due to this effect. For this reason we have put the numbers into brackets, and we do not yet consider significant the difference in the cross section between the points for $K = 978$ MeV and for $K = 938$ MeV. For the evaluation of the errors in the cross section the solid angle (in both spark chamber and counter measurements) was considered known with 10% accuracy.

Multipion background. -

The point has been already discussed in § 3. As we already pointed out, the background contaminates mainly the $\eta \rightarrow 3\pi^0$ ($\eta \rightarrow \pi^0 + \mathcal{J} + \mathcal{J}$) measurements.

The error in the extrapolation of the background was included in the statistical one and propagated to the branching ratio and cross sections.

All the multipion background measurements were made with the aid of the spark chamber. The uncertainty in the solid angle for the non-spark-chamber measurements give thus rise to an uncertainty in the evaluation of the absolute rate of the multipion background for those measurements, and therefore in the determination of the $\eta \rightarrow 3\pi^0$ ($\eta \rightarrow \pi^0 + \mathcal{J} + \mathcal{J}$) contribution. For this reason the values of branching ratio of rows 3 and 4 of Table I have been put into brackets, and not used to obtain the average value R.

Nuclear absorption of the protons. -

The correction for nuclear interactions of the protons is as high as $\sim 50\%$. An error in the estimate of this correction affects the cross sections but not the branching ratios. For this correction a mean free path in Al for nuclear interaction of 115 gr/cm^2 was used. This was obtained by using the experimental information from the measurements of Milburn et al. (21).

A similar correction with the same assumption was applied for a measurement previously done with the same proton telescope on single π^0 photoproduction⁽⁴⁴⁾: we are confident that this correction is quite all-right, since the absolute values of the cross section for single π^0 photoproduction we obtained agrees fairly well (5-10%) with the results of magnet measurements done by other authors⁽⁴⁵⁾. Anyway a 10% error in the cross sections was considered possible owing to an error in the evaluation of this correction.

Other sources of errors were considered, but we do not quote them since they were found small with respect to the ones discussed.

Appendix 2 - CALIBRATION OF THE CERENKOV C. -

The Cerenkov counter is a solid lead glass cylinder. The lead glass is viewed by three Philips 58AVP, 5" photomultipliers connected in parallel. At the entrance of the Cerenkov a lead ring fixes the aperture of the counter toward the H₂ target to a diameter of 25 cm.

The calibration of the lead glass Cerenkov (see Section 1 and fig. 1) has been done by sending to C a beam of monochromatic electrons at various energies. The beam was taken at the exit of the Frascati pair spectrometer⁽¹⁸⁾. This calibration may be considered as valid for the photons. In fact the initial difference (a photon rather than an electron) will only display the development

of the shower in the lead glass, while the length of our Cerenkov (~ 12 radiation lengths) is enough to absorb all the cascade shower in the range of energies (200-700 MeV) covered in our measurements.

Experimental disposition for the calibration. -

The disposition for the calibration is given in fig. 13. The bremsstrahlung spectrum from the synchrotron (the energy of the machine was set at 1000 MeV) is collimated in the lead collimators C_1 and C_2 . Use is made of a

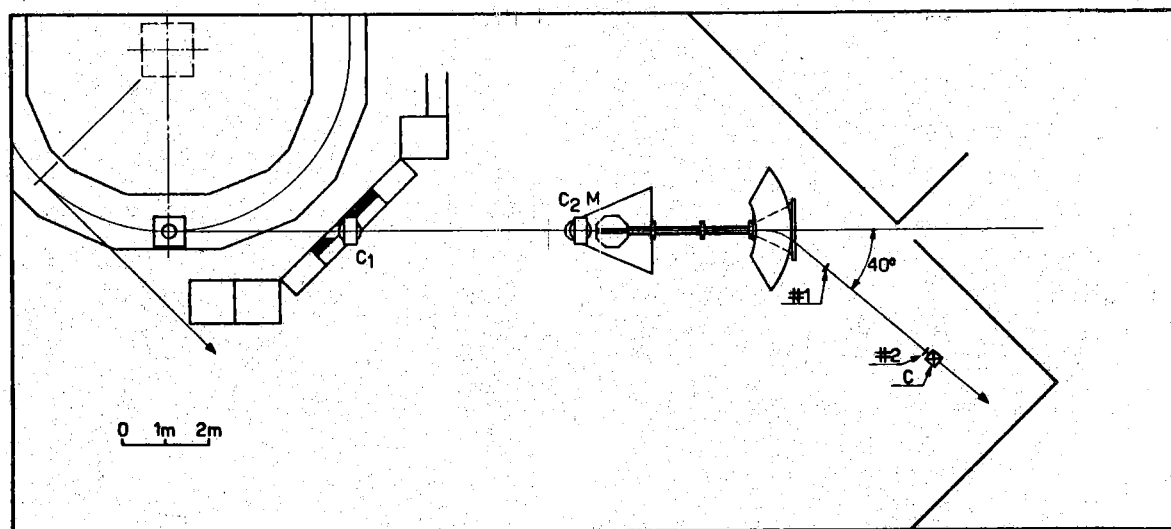


FIG. 13 - Experimental set-up for the Cerenkov calibration.

sweeping magnet M to eliminate contaminating electrons in the beam. The bremsstrahlung beam travels in vacuum in the way from M to the converter. The gap of the spectrometer is also under vacuum. The converter producing the electron pairs at the entrance of the spectrometer is an Aluminum disk of different thickness from 0.1 to 1 mm (0.1 mm in the case of fig. 14). Once the Cerenkov was placed at a given exit angle θ from the spectrometer the energy of the electrons hitting the Cerenkov was changed by varying the magnetic field in the spectrometer. The angle θ is fixed to 40° by the counters 1 ($10 \times 10 \text{ cm}^2$) and 2 ($5 \times 5 \text{ cm}^2$) (see fig. 13). In these conditions the spectrum of the electrons entering the Cerenkov is rather well defined around the average energy E : in fact it is flat with a width $\delta E/E = \pm 2\%$.

All the electronics used in the calibration from the Cerenkov to the analyzer was the same as we employed with the actual measurement of the η .

Results of the calibration. -

The pulse height distributions from the Cerenkov are reported in fig. 14 for different energies of the electron beam. We see, as expected, that the abscissae of the peaks of these distributions are linearly correlated to the energy of the electron beam entering the Cerenkov. This appears clearly in fig. 15 where the peak position in the multichannel is plotted versus the electron energy.

As we can estimate from fig. 14, the relative width $\Delta E/E$ of the pulse height spectrum is always less than 30%. The values of the absolute widths

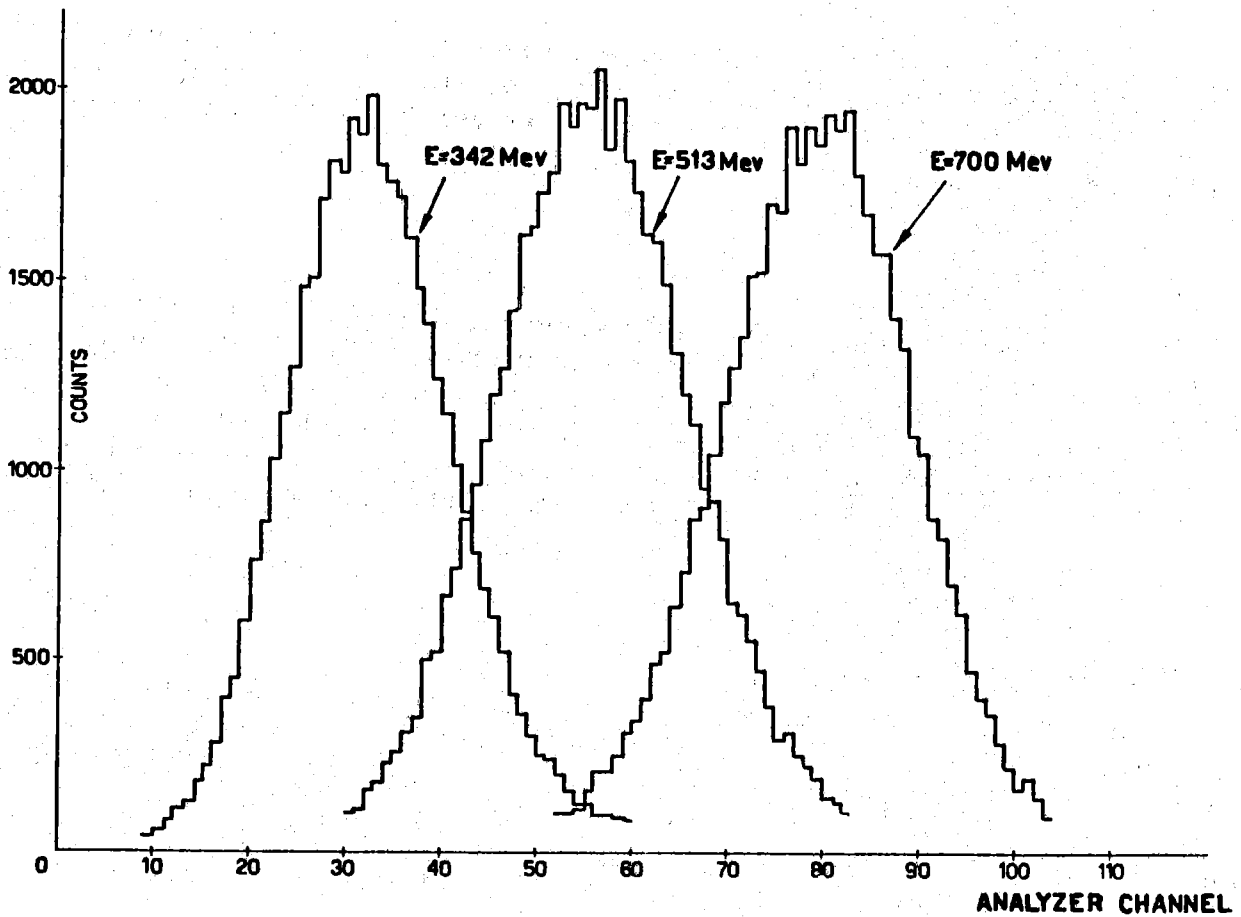


FIG. 14 - Typical pulse height distributions from the Cerenkov for different energy incident electron beams.

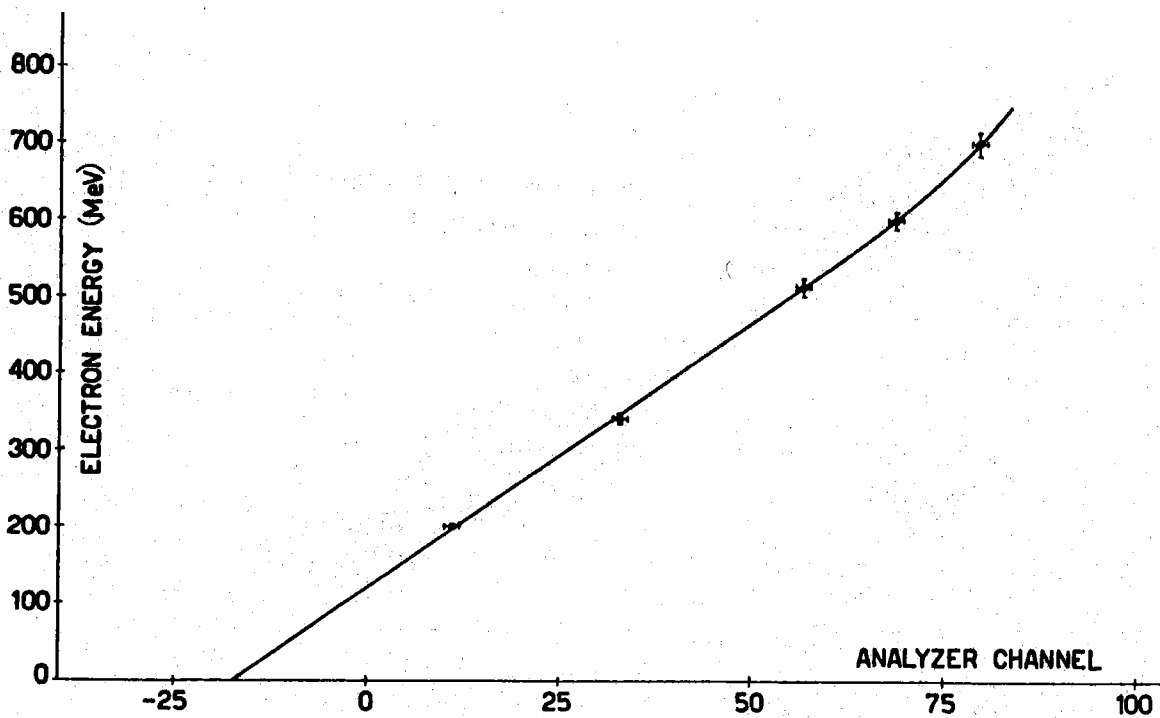


FIG. 15 - Results of the calibration of the Cerenkov counter: average energy of the electron beam incident on the Cerenkov vs analyzer channel at which the pulse-height distribution is centered.

ΔE fix the resolution of the Cerenkov C at each energy. By illuminating with electrons different regions of the Cerenkov C and by slightly rotating the axis of the Cerenkov with respect to incident beam, we verified that each pulse height distribution of fig. 14 did not change appreciably.

Stability of the Cerenkov calibration. -

By repeating our calibration with some regularity we found some slight ($<10\%$) and slow variations of the calibration of the constants (position of the peak and width). These changes were taken continuously under control and corrected by systematic measurements of the pulse height distribution of the cosmic ray particles hitting the Cerenkov. This almost continuous inspection resulted to be a powerful check particularly convenient in our case.

ACKNOWLEDGMENTS. -

During all of our measurements, particular care was to be taken in the synchrotron operation to keep constant beam intensity and energy. We are indebted to the machine staff for providing us a beam whose reliability and intensity was always very good, and for technical assistance in all our problems.

Thanks are due to the cryogenics group for H₂ target construction and operation.

We are indebted to Profs. Cabibbo, Ferrari, Gatto and Vitale and to Dr. Holloway for many illuminating discussions on the theoretical interpretation of the results.

REFERENCES. -

- (1) - A. Pevsner, R. Kraemer, N. Nussbaum, C. Richardson, P. Schlein, R. Strand, T. Toohig, M. Block, A. Engler, R. Gessaroli and C. Melzer, Phys. Rev. Letters 7, 421 (1961).
- (2) - P. L. Bastien, J. P. Berge, O. I. Dahl, M. Ferro-Luzzi, D. H. Miller, J. J. Murray, A. H. Rosenfeld and M. B. Watson, Phys. Rev. Letters 8, 114 (1962).
- (3) - H. Foelsche, E. C. Fowler, H. L. Kraybill, J. R. Sanford and D. Stonehill, Proc. of the Int. Conf. on High Energy Nuclear Physics, Geneva 1962, pag. 36.
- (4) - T. Toohig, R. Kraemer, L. Madansky, M. Meer, M. Nussbaum, A. Pevsner, C. Richardson, R. Strand and M. Block, Proc. of the Int. Conf. on High Energy Nuclear Physics, Geneva 1962, pag. 99.
- (5) - M. Meer, R. Strand, R. Kraemer, L. Madansky, M. Nussbaum, A. Pevsner, C. Richardson, T. Toohig, M. Block, S. Orenstein and T. Fields, Proc. of the Int. Conf. on High Energy Nuclear Physics, Geneva 1962, pag. 103.

- (6) - M. C. Foster, M. L. Good, R. P. Matson, M. W. Peters, G. W. Taurfest and R. B. Willman, Proc. of the Int. Conf. on High Energy Nuclear Physics, Geneva 1962, pag. 108.
- (7) - E. Pickup, D. K. Robinson and E. O. Salant, Phys. Rev. Letters 8, 329 (1962).
- (8) - C. Alff, D. Berley, D. Colley, N. Gelfand, U. Nauenberg, D. Miller, J. Schultz, J. Steinberger, T. H. Tan, H. Brugger, P. Kramer and R. Plano, Phys. Rev. Letters 9, 322 (1962); 9, 325 (1962).
- (9) - E. C. Fowler, R. S. Crawford, L. J. Lloyd, R. A. Grossman, LeRoy Price, and experiments quoted by these authors, Phys. Rev. Letters 10, 110 (1963).
- (10) - D. D. Carmony, A. H. Rosenfeld and R. T. Van de Walle, Phys. Rev. Letters 8, 117 (1962).
- (11) - D. D. Carmony, A. H. Rosenfeld and R. T. Van de Walle, Phys. Rev. Letters 8, 293, (1962).
- (12) - C. Mencuccini, R. Querzoli, G. Salvini and V. Silvestrini, Proc. of the Int. Conf. on High Energy Nuclear Physics, Geneva 1962, pag. 33.
- (13) - M. Chrétien, F. Bulos, H. R. Crouch, R. E. Lanon, J. T. Massimo, A. M. Shapiro, J. A. Averell, C. A. Bordner, A. E. Brenner, D. R. Firth, M. E. Law, E. E. Ronat, K. Strauch, J. C. Street, J. J. Szymanski, A. Weinberg, B. Nelson, I. A. Pless, L. Rosenson, G. A. Salandin, R. K. Yamamoto, L. Guerriero and F. Waldner, Phys. Rev. Letters 9, 127 (1962).
- (14) - C. Bacci, G. Penso, G. Salvini, A. Wattenberg, C. Mencuccini, R. Querzoli and V. Silvestrini, Proc. of the Conf. on Photon Interactions in the BeV-energy Range, Cambridge (1963), IV. 6. We reported a preliminary value $R = \eta \rightarrow \pi\pi / \eta \rightarrow 3\pi^0 = 1.0 \pm 0.5$.
- (15) - F. S. Crawford, D. G. Loyd and E. C. Fowler, Phys. Rev. Letters 10, 546 (1963).
- (16) - C. Bacci, G. Penso, G. Salvini, A. Wattenberg, C. Mencuccini, R. Querzoli and V. Silvestrini, Phys. Rev. Letters 11, 37 (1963).
- (17) - R. R. Wilson, Nuclear Instr. 1, 101 (1957).
- (18) - G. Bologna, G. Diambrini and G. P. Murtas, Suppl. Nuovo Cimento 24, 342 (1962).
- (19) - M. M. Block, Phys. Rev. 101, 796 (1956).
- (20) - R. Querzoli and V. Silvestrini, Laboratori Nazionali di Frascati, LNF 62/59 (1962).
- (21) - G. P. Millburn, W. Birnbaum, W. E. Crandall and L. Schechter, Phys. Rev. 95, 1268 (1954).
- (22) - M. Gell-Mann, D. Sharp and W. G. Wagner, Phys. Rev. Letters 8, 261 (1962).
- (23) - A. Muller, E. Pauli, R. Barloutaud, L. Cardin, J. Meyer, M. Beneventano, G. Gialanella and L. Paoluzi, The Sienna Int. Conf. on Elementary Particles (1963), pag. 99.
- (24) - S. Okubo and B. Sakita, Phys. Rev. Letters 11, 50 (1963).
- (25) - K. Berkelman, A. Franklin, D. McLeod, S. Richert and A. Silverman, Nuovo Cimento, 27, 497 (1963).
- (26) - B. Delcourt, J. Lefrançois, J. P. Perez Y Jorba and J. K. Walker, Phys. Rev. Letters 7, 215 (1963).
- (27) - L. M. Brown and P. Singer, Phys. Rev. Letters 8, 460 (1962).
- (28) - E. Ferrari and L. Holloway, Istituto di Fisica dell'Università di Roma, Nota interna n. 32.

- (29) - According to a detailed calculation of Ferrari and Holloway⁽²⁸⁾ the theoretical value of this branching ratio should be lower by a factor 4 respect to the estimate of Brown and Singer⁽²⁷⁾.
- (30) - G. Barton and S. P. Rosen, Phys. Rev. Letters 8, 414 (1962).
- (31) - D. A. Geffen, Phys. Rev. 128, 374 (1962).
- (32) - G. Barton, Nuovo Cimento 27, 1179 (1963).
- (33) - M. A. B. Beg and P. De Celles, Phys. Rev. Letters 8, 46 (1962).
- (34) - D. Berley, D. Colley and J. Schultz, Phys. Rev. Letters 10, 114 (1963).
- (35) - L. M. Brown and P. Singer, to be published.
- (36) - M. A. B. Bég, Phys. Rev. Letters 9, 67 (1962). We recall that some general properties interesting the are contained in some theorems demonstrated by G. Feinberg and A. Pais, Phys. Rev. Letters 9, 45 (1962).
- (37) - K. C. Wali, Phys. Rev. Letters 9, 120 (1962).
- (38) - C. Kacser, Phys. Rev. 130, 355 (1963).
- (39) - F. S. Crawford, J. Ronald, A. Grossman, L. J. Lloyd, Le Roy, R. Puce, and E. C. Fowler, Phys. Rev. Letters 11, 564 (1963).
- (40) - Riazuddin and Fayyazuddin, Phys. Rev. 129, 2337 (1963).
- (41) - B. Barret and G. Barton, Phys. Letters 4, 16 (1963).
- (42) - N. Cabibbo and R. Gatto, Nuovo Cimento 21, 872 (1961).
- (43) - J. B. Bronzan and F. E. Low, The Sienna Int. Conf. on Elementary Particles (1963), pag. 450.
- (44) - M. Deutsch, C. Mencuccini, R. Querzoli, G. Salvini, V. Silvestrini and R. Stiening, Proc. of the Aix-en-Provence Conf. on Elementary Particles (1961), Vol. I, Pag. 9.
- (45) - R. E. Diebold, Thesis (California Institute of Technology, unpublished).